10-30-2020

Testing the Circadian Regulation of the JAK/STAT Signaling Pathway

Daniela Bianca Bachetti
University of Windsor

Testing the Circadian Regulation of the JAK/STAT Signaling Pathway

By

Daniela Bianca Bachetti

A Thesis
Submitted to the Faculty of Graduate Studies
Through the Department of Integrative Biology
In Partial Fulfillment of the Requirements
For the Degree of Master of Science at the University of Windsor

Windsor, Ontario, Canada

2020

Testing the Circadian Regulation of the JAK/STAT Signaling Pathway

By

Daniela Bianca Bachetti

APPROVED BY:

S. Pandey
Department of Chemistry and Biochemistry

A. Swan
Department of Biomedical Sciences

P. Karpowicz, Advisor
Department of Biomedical Sciences

August 31, 2020

DECLARATION OF ORIGINALITY

I hereby certify that I am the sole author of this thesis and that no part of this thesis has been published or submitted for publication.

I certify that, to the best of my knowledge, my thesis does not infringe upon anyone's copyright nor violate any proprietary rights and that any ideas, techniques, quotations, or any other material from the work of other people included in my thesis, published or otherwise, are fully acknowledged in accordance with the standard referencing practices. Furthermore, to the extent that I have included copyrighted material that surpasses the bounds of fair dealing within the meaning of the Canada Copyright Act, I certify that I have obtained a written permission from the copyright owner(s) to include such material(s) in my thesis and have included copies of such copyright clearances to my appendix.

I declare that this is a true copy of my thesis, including any final revisions, as approved by my thesis committee and the Graduate Studies office, and that this thesis has not been submitted for a higher degree to any other University or Institution.

ABSTRACT

Many organisms coordinate behavioural and physiological processes with the Earth's 24-hour light/dark cycle. This cycle, the circadian rhythm, is anticipated by the circadian clock, a 24-hour timekeeper that is comprised of a transcription-translation feedback loop. The clock regulates the transcription of genes, which can influence the expression of oscillating circadian behaviours, such as sleep/wake. Maintaining tissue homeostasis is an important process, especially in tissues with high cellular turnover rates, such as the intestine. Involved in this intestinal regenerative response is the Janus Kinase/Signal Transducer and Activator of Transcription (JAK/STAT) pathway. Damaged cells or exposure to a stressful environment will activate the JAK/STAT pathway to cause increased division of intestinal stem cells and increased differentiation of enteroblasts. Previous work has indicated that intestinal stem cells possess circadian clock activity and the clock regulates intestinal stem cell division during regeneration, suggesting a link between the JAK/STAT regenerative response and the circadian clock. This thesis shows that the circadian clock regulates a time of day dependent damage response in the intestine, and under undamaged conditions, period regulates the JAK/STAT response in the intestine in a non-time dependent manner. Additionally, my research shows that bacterial presence is required to elicit a damage response and axenically raised flies can suppress this response. My research establishes the first link between the circadian clock and the JAK/STAT pathway.

ACKNOWLEDGEMENTS

I would like to thank the University of Windsor, the National Sciences and Engineering Council of Canada (NSERC) and the Government of Ontario for funding my research project. I would also like to thank my parents, Brenda and Joe, and my sister, Julia, their continued support and for always believing in me throughout the duration of my project. I am thankful for the guidance and wealth of knowledge Dr. Phillip Karpowicz has shared during this project. I am also grateful for the feedback and suggestions given to me from my committee members- Dr. Andrew Swan and Dr. Siyaram Pandey. Lastly, I would like to thank the members of the Karpowicz lab—especially Kathyani Parasram, for being one of my *Drosophilist* mentors and teaching me your tips and tricks throughout this project, and our lab manager Sharon Lavigne-Yong—for all their continued encouragement and for sharing all the memories that I will cherish forever.

TABLE OF CONTENTS

LIST OF TABLES

LIST OF FIGURES

LIST OF ABBREVIATIONS

Cat. no. ……..	Catalogue Number
CLK……	Clock
CRY……	Cryptochrome
CT……...	Circadian Time
CYC……	Cycle
DAPI……...	4’,6-diamidino-2-phenylindole
D:D…….	Dark: Dark
dGFP……...	Destabilized Green Fluorescent Protein
dH_2O……...	Distilled Water
DHE……	Dihydroethidium
DMSO……	Dimethyl Sulfoxide
DNA……..	Deoxyribonucleic Acid
DSS……	Dextran Sulfate Sodium
GFP……	Green Fluorescent Protein
JAK/STAT…….	Janus Kinase/ Signal Transducer and Activator of Transcription
JNK…….	c-Jun N-Terminal Kinase
L:D……..	Light: Dark
n.s. ……..	Not Significant
PBS……....	Phosphate Buffer Solution
PER…….	Period
PFA…….	Paraformaldehyde
R……..	Region
ROS…….	Reactive Oxygen Species
SEM……	Standard Error of the Mean
TIM…….	Timeless
TSA…….	Tryptic Soy Agar
UPD…….	Unpaired
YKI……..	Yorkie
ZT……	Zeitgeber Time

CHAPTER 1

INTRODUCTION

1.1 Circadian Rhythms

Many organisms coordinate behavioural and physiological processes with the Earth's 24-hour light/dark cycle. This cycle, known as the circadian rhythm, is controlled internally by an endogenous oscillator, the circadian clock. Circadian rhythms are 24-hour cycles that can: be entrained by environmental cues (such as photoperiod), persist in the absence of cues and are temperature compensated (Panda *et al.*, Nature, 2002). Circadian rhythms can influence various health-related processes, such as sleep/wake cycles, release of hormones and eating habits (Serin & Acar Tek, Ann Nutr Metab, 2019; Farhud & Aryan, Iran J Public Health, 2018), and disruptions to the circadian rhythm could result in negative health-related outcomes.

The circadian rhythm is an endogenous timekeeper, which allows organisms to anticipate and appropriately react to day and night changes in the environment (Panda *et al.*, Nature, 2002). An important feature of circadian rhythms is that they continue to persist in the absence of external cues, such as light (Panda *et al.*, Nature, 2002). Disruptions to one's circadian rhythm, such as jet lag or shift work, have been shown to have negative consequences on health and increased risk of illnesses. A study on sleep restricted participants was performed and after five nights of sleep restriction, the participants' insulin levels were reduced by 24%, implicating glucose metabolism as a metabolic consequence of circadian disruption (Spiegel *et al*., Lancet, 1999). This is especially relevant for the Windsor-Essex region because many residents are scheduled shift work and may not be aware of the adverse effects it may have on their overall health and well-being. Research over the years has implicated various diseases and attributed decreased fitness to organisms that disrupt their circadian rhythm. A study subjecting mice to circadian

disruptions showed an increased risk of developing Type Two Diabetes Mellitus (Gale *et al.,* J Biol Rhythms, 2011). Another study performed in mice revealed a correlation between desynchrony of the circadian rhythm and the increased risk of cancer progression and tumorigenesis (Savvidis & Koutsilieris, Mol Med, 2012). Thus, incorporation of circadian rhythm considerations may benefit the fitness or well-being of one's overall health to avoid circadian-related diseases.

1.2 The Circadian Clock

The clock is a transcription-translation feedback loop consisting of a repressor and an activator to regulate transcription (Hardin, Adv Genet, 2011). In *Drosophila melanogaster,* it is made up of two main components (i) CLK-CYC, which is the activator and (ii) PER-TIM, which is the repressor (Figure 1). CLK and CYC circadian transcription factors will heterodimerize and form a CLK-CYC complex (Lee *et al.,* Mol Cell Biol, 1999). The CLK-CYC complex will attach to the enhancer box (E-box) to promote the transcription of PER and TIM (Lee *et al.,* Mol Cell Biol, 1999). During the night, PER and TIM will accumulate and form heterodimers with one another. The PER-TIM complex will promote the phosphorylation of CLK-CYC by entering into the nucleus (Lee *et al.,* Mol Cell Biol, 1999). Phosphorylation of CLK-CYC will reduce its affinity for DNA, thereby inhibiting its activity.

This clock mechanism continues to regulate transcription even in the absence of external cues, such as light (Parasram & Karpowicz, Cell Mol Life Sci, 2019), allowing the circadian clock to cycle in 24-hour oscillations. This feature of the circadian clock can be easily manipulated when using *Drosophila* as a model organism. Under normal conditions, *Drosophila* are exposed to light:dark conditions (LD) of 12 hours of light and 12 hours of darkness, known

as Zeitgeber Time (ZT). For day active organisms, the time that the lights turn on is denoted as ZT0. After 12 hours, the lights will turn off and this time is denoted as Z12. At this point, after an additional 12 hours, the cycle will begin again at ZT0. To test if a rhythm or process is truly circadian, following appropriate LD synchronization, *Drosophila* can be moved to complete darkness (DD). The circadian nomenclature changes to Circadian Time (CT), which is used to denote free running conditions. Shifting the flies to DD conditions following synchronization can provide insight to the circadian aspect of that rhythm, because LD conditions only provide information on time of day differences. Any rhythms noted in the absence of external cues may be a result of previous entrainment of the endogenous time-keeper (Dubowy & Sehgal, Genetics, 2017).

FIGURE 1

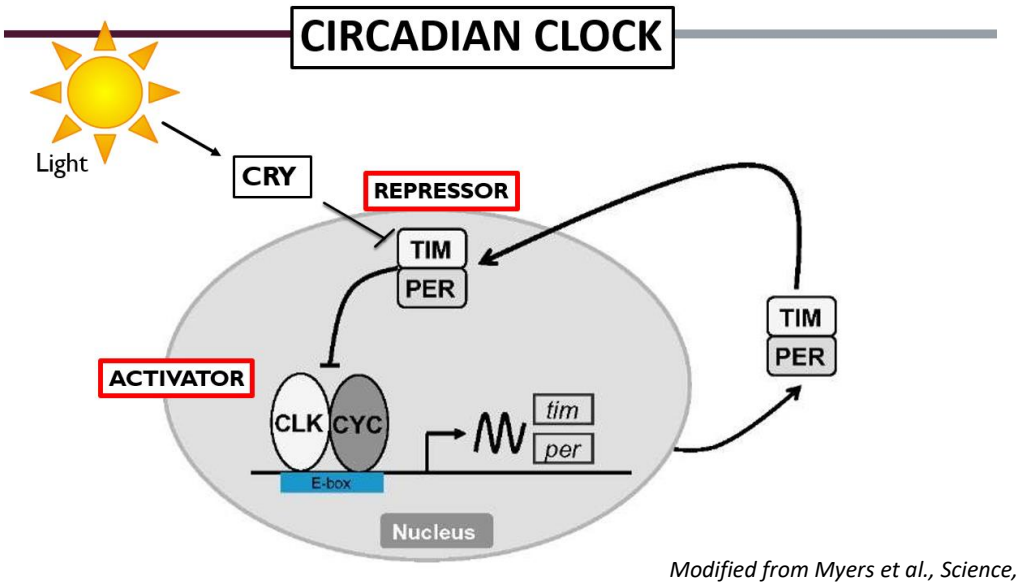

Modified from Myers et al., Science, 1995

Figure 1: Schematic of the Circadian Clock Mechanism in *Drosophila*

Light is the strongest circadian synchronizer and it has the ability to shift the circadian clock so that the clock can be entrained to differently timed light/dark cues (Castillo *et al*., Am J Physiol-Reg I, 2004). *Drosophila* are able to detect light with all their cells because every cell has a Cryptochrome (CRY) protein that is sensitive to light (Busza *et al.*, Science, 2004). A brief light pulse activates CRY, allowing it to bind to TIM (Allada & Chung, Annu Rev Physiol, 2010). Once bound, TIM will be rapidly degraded through ubiquitination and proteasomal degradation thereby permitting the release of CLK-CYC from repression (Hardin, Adv Genet, 2011; Yoshii *et al.*, J Neurosci, 2015). This degradation process allows for the synchronization of the circadian rhythm to shift and be altered (for example, jet lag).

1.3 Life Cycle of Drosophila

Drosophila melanogaster have a relatively large brood size, short lifespan and short generation time making them an ideal model organism, especially for genetic studies. Typically, *Drosophila* are raised at 25^{o}C, and the generation time is approximately ten days to go from fertilized egg to an eclosed (hatched) adult (Fernandez-Moreno *et al.*, Methods Mol Biol, 2007). If raised at lower temperatures, such as 18^{o}C, the generation time will be slightly delayed. The four main stages of its life cycle are embryo, larva, pupa and adult. The first stage is embryogenesis and this stage usually only lasts 24-hours (Fernandez-Moreno *et al.*, Methods Mol Biol, 2007). From here, the embryo will become a first instar larva, where it will remain on the surface of food and will begin eating. After one day, the first instar larva will molt into a second instar larva (Fernandez-Moreno *et al.*, Methods Mol Biol, 2007) and it will begin to burrow into the food. After another day, the second instar larva will molt into a third instar larva. A matured late stage third instar larva will begin to crawl up along the sides of the vial

until the larva finds a suitable place to pupariate. This usually takes 60 to 72 hours (Fernandez-Moreno *et al.,* Methods Mol Biol, 2007). During the pupal stage, complete metamorphosis will occur resulting in the degradation of most larval tissues permitting adult organs to develop from undifferentiated cells (Fernandez-Moreno *et al.,* Methods Mol Biol, 2007). The pupal stage usually lasts three and a half to four and a half days. Figure 2 illustrates a schematic of the *Drosophila* life cycle. Following pupation, the fly will eclose into an adult *Drosophila*. The intestine continues to develop and will not stabilize until approximately adult day three (Takashima *et al.*, Nature, 2011).

FIGURE 2

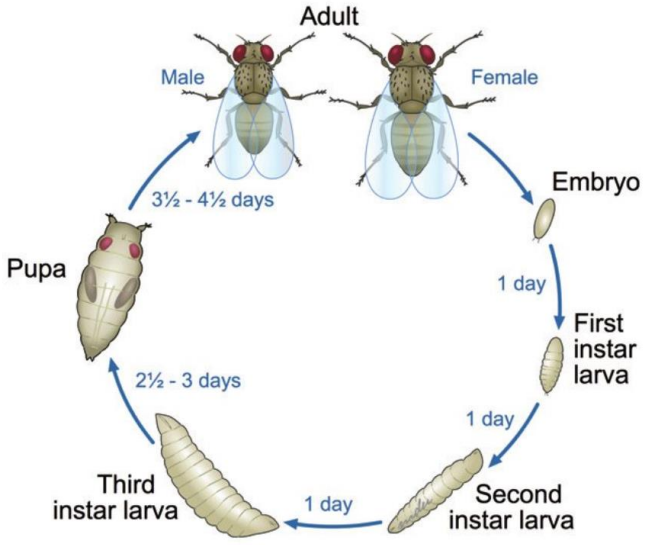

Image Taken from: Ong et. al, Nanotoxicity, 2015

Figure 2: Life Cycle of *Drosophila melanogaster*
Illustration of the typical life cycle of the *Drosophila melanogaster*, commencing from the embryo stage to its adult stage.

1.4 Drosophila Intestinal Anatomy, Regionalization and Model for Regeneration

The *Drosophila* intestine has functions in digestion, nutrient absorption, and protection against pathogens (Hung *et al.*, PNAS, 2020). The *Drosophila* intestine is a simple epithelium composed of four main types of cells: intestinal stem cells, enteroblasts, enterocytes and enteroendocrine cells. As shown in Figure 3, self-renewing intestinal stem cells produce either more intestinal stem cells or enteroblast progenitors that go on to differentiate into enterocytes (absorptive cells) and enteroendocrine cells (secretory cells), [Micchelli & Perrimon, Nature (Letters), 2006; Ohlstein & Spradling, Nature (Letters), 2006]. Recent research from our lab (Parasram *et al.*, Stem Cell Rep, 2018) tested the circadian activity in all four cell types at different times of day to determine if they exhibited clock reporter activity. It was determined that three of the cell types, intestinal stem cells, enteroblasts and enterocytes, all contain clock reporter activity. Surprisingly, it was determined that enteroendocrine cells do not exhibit clock activity suggesting clock activity is turned off during enteroendocrine cell differentiation.

FIGURE 3

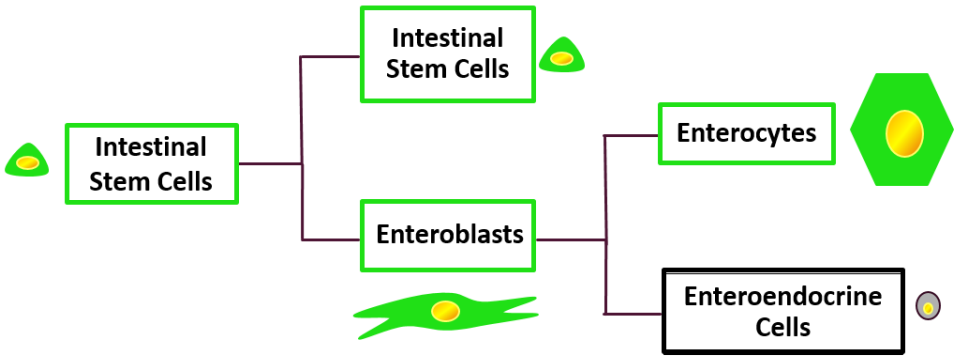

Adapted from Parasram et al., Stem Cell Rep, 2018

Figure 3: Schematic of Main Cell Types in the *Drosophila* Intestine
Image shows the four main types of cells within the *Drosophila* intestine: intestinal stem cells, enteroblasts, enterocytes and enteroendocrine cells. The intestinal stem cells, enteroblasts and

enterocytes have been shown to have clock activity (outlined in green) while the enteroendocrine cells do not have clock activity (outlined in black) (Parasram *et al.*, Stem Cell Rep, 2018). Note that the images are not illustrated to scale.

Cell morphology and function vary greatly throughout the *Drosophila* intestine. In 2013, Buchon and colleagues (Cell Reports) identified five distinctive regions of the adult intestinal midgut and named them Region (R) 1, R2, R3, R4 or R5, where R1 is the most anterior portion and R5 is the most posterior portion of the midgut. The R1 region is mainly composed of flat and long enterocytes. The R2 region is mostly composed of enterocytes containing lipid vesicles. The R3 region consists of the copper cell region and large flat cells. The R4 region consists of mostly enterocytes and the anterior portion of R4 is often highly folded. Lastly, the R5 region contains fewer cells with a brushed border. Marianes & Spradling (eLife) also released their work on regionalization in 2013, and they further subdivided each region. For simplicity, the R1 to R5 regional compartmentalization system was followed for this project. Figure 4 shows a schematic of the *Drosophila* intestinal midgut characterization.

FIGURE 4

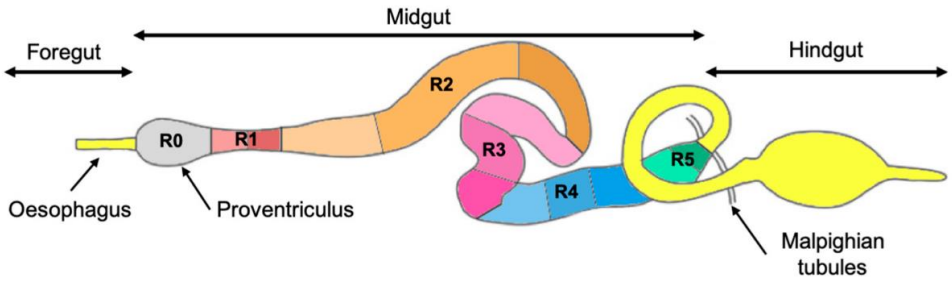

Taken from Capo et al., Microorganisms, 2019

Figure 4: *Drosophila* Intestinal Region Compartmentalization
Illustration of the compartmentalization of the *Drosophila* midgut from regions R1 (most anterior) to R5 (most posterior).

As previously mentioned, *Drosophila* is an ideal model organism to investigate intestinal physiology. Through intestinal stem cells, the intestinal epithelium is renewed every one to two weeks (Buchon *et al.*, Cell Reports, 2013). Due to the frequent renewal of the intestinal epithelium, the adult intestine is an appropriate organ to study cellular regeneration. Additionally, mammalian intestinal diseases can be modelled successfully in *Drosophila* with findings that can be translatable to humans because of the high degree of conservation between the signaling pathways, such as pathways that control intestinal development, regeneration and disease, in both humans and *Drosophila* (Apidianakis & Rahme, Dis Model Mech, 2011).

1.5 JAK/STAT Signaling Pathway and Reporter

An important signaling pathway that regulates intestinal stem cells is the Janus Kinase/ Signal Transducer and Activator of Transcription (JAK/STAT) pathway, which is vital for their proliferation and maintenance (Lin *et al*., J Mol Cell Biol, 2010) as well as differentiation of the intestinal progenitor cells (Muller *et al.*, Nature, 2005). Damaged cells or exposure to a stressful environment will trigger enterocytes to produce unpaired (UPD) cytokines, which activate the JAK/STAT signaling pathway causing increased division of intestinal stem cells and increased differentiation of enteroblasts to promote enterocyte replacement (Beebe *et al.*, Dev Bio, 2010; Jiang *et al.*, Cell, 2009). The JAK/STAT pathway is homologous to the mammalian signal transducer and activator of transcription 3 (STAT3) signaling pathway, where interleukin-6 cytokine induces an inflammatory response when the intestine is under stressful conditions [Biteau *et al.*, Cell Stem Cell (Review), 2011; Panayidou & Apidianakis, Pathogens, 2013]. Along with the *Drosophila* intestine, the JAK/STAT signaling pathway also has regenerative roles in the *Drosophila* testes and the *Drosophila* wing disc (Herrera & Bach, Development,

2018). Previous work in the lab has indicated that the circadian clock regulates intestinal stem cell division during regeneration, and that the JAK/STAT pathway may be under circadian clock control (Karpowicz *et al.*, Cell Rep, 2013).

The mechanistic process of the JAK/STAT pathway is illustrated in Figure 5. The UPD cytokines released from the enterocytes will bind to the domeless receptor, bringing the domeless receptors closer in proximity [Arbouzova & Zeidler, Dev (Review), 2006]. This allows for two JAK molecules to trans-phosphorylate one another [Arbouzova & Zeidler, Dev (Review), 2006]. Once phosphorylated, the activated JAK molecules will phosphorylate the tyrosine kinases on the cytokine receptor [Arbouzova & Zeidler, Dev (Review), 2006]. The phosphorylated tyrosine kinases will recruit and bind SH2 (Src Homology 2) domains, which allows for the phosphorylation of the STAT molecules [Arbouzova & Zeidler, Dev (Review), 2006]. This permits the STAT molecules to dissociate from the domeless receptor and dimerize with one another [Arbouzova & Zeidler, Dev (Review), 2006]. The dimerized STAT molecule will translocate into the nucleus and bind to an E-box to promote the transcription of various target genes, such as SOCS36E (suppressor of cytokine signalling) [Arbouzova & Zeidler, Dev (Review), 2006]. The molecular aspects to this mechanism are well studied, but there is still a gap in the literature with respect to possible clock control of this pathway.

FIGURE 5

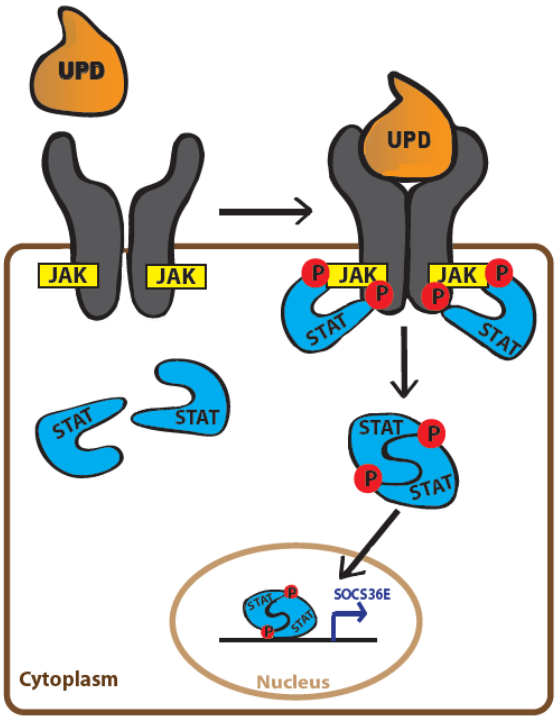

Adapted from Arbouzova & Zeidler, Dev (Review), 2006

Figure 5: JAK/STAT Mechanism in *Drosophila* Schematic

A 6XSTAT-dGFP reporter was used to investigate the JAK/STAT activity levels *in vivo* (He *et al.*, eLife, 2019) (Figure 6). There are two main components to this reporter (i) a destabilized green fluorescent protein (dGFP) and (ii) a PEST domain. This reporter contains six copies of the SOCS36E promoter, in tandem, upstream of a superfolder dGFP. dGFP transcription will simultaneously be driven if the STAT92E protein binds to the SOCS36E promoter. The dGFP is fused to a PEST domain, which signals the protein degradation (He *et al.*, eLife, 2019). As a result, if a cell fluoresces green (GFP+), that means that cell is reporting STAT transcriptional activity from within the last hour (He *et al.*, eLife, 2019).

FIGURE 6

Taken from K. Parasram, unpublished

Figure 6: 6XSTAT-dGFP Reporter
Construction of the 6XSTAT-dGFP reporter illustrating the 6 x minimal promoter sequence upstream of a dGFP.

To be able to visualize clock activity *in vivo*, a clock reporter was constructed by our lab group (Parasram *et al*, Stem Cell Rep, 2018). It contains four copies, in tandem, of the minimal promoter from the clock target, *per* (Figure 7). The minimal promoter contains a 123 base pair sequence which includes E-box and W-box binding sites for the CLK/CYC dimer. Simultaneous transcription of Clock^{PER} and a GFP molecule occur once the CLK/CYC dimer binds to the promoter region of *per*. Clock activity could be dynamically measured over time due to the fusion of the PEST domain to a GFP molecule in the reporter. This PEST domain is a peptide signal for protein degradation, so it causes the GFP signal to degrade shortly after it is produced (He *et al*., eLife, 2019). Thus, the dGFP will give transcriptional information within the last hour before it gets degraded.

FIGURE 7

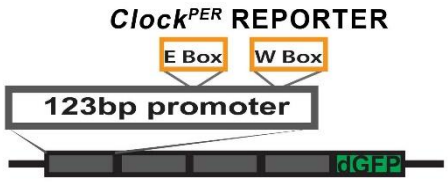

Taken from Parasram et al., Stem Cell Rep, 2018

Figure 7: Clock^{PER} Reporter
Illustration of the Clock^{PER} reporter depicting the 4 x minimal promoter sequence upstream of a dGFP.

1.6 JNK and Hippo Pathways in Cellular Proliferation and the Stress Response

The JNK and Hippo pathways are two signaling pathways that are also both involved in cellular proliferation and the stress response. The JNK pathway can respond to stressors such as infection, inflammation and oxidative stress (Zeke *et al.*, Microbiol Mol Biol R, 2016). The Hippo pathway has been shown to have roles in apoptosis and stem cell renewal. The YKI gene is a transcriptional coactivator in *Drosophila*, and stress signals, such as cellular damage, can activate the Hippo pathway (Boopathy & Hong, Front Cell Dev Biol, 2019). In this thesis, I primarily studied the JAK/STAT pathway, but reporters of these two were also initially examined and some data is presented for this work.

1.7 Hypothesis

I hypothesized that the timing of the adult *Drosophila* intestinal stress response is regulated by the circadian clock.

This thesis project was designed to explore three main questions. First, an acute damage assay needed to be created and optimized so that the possible effects from acute damage could be

assessed regarding cellular morphology, changes in the stress response (via the JAK/STAT reporter) and survival. The acute damage assay I eventually used was x-ray irradiation. The next question set out to determine if the JAK/STAT pathway, Hippo pathway or JNK pathway is under 24-hour circadian clock control, and if so, determine if the intestinal stress is a direct result of the damage caused by irradiation or an indirect effect of the irradiation on bacteria in the intestine, leading to an inflammatory response. Only the JAK/STAT pathway was developed. Timed circadian response to damage was tested by administering the irradiation at different times of day. This assay was taken one step further and repeated using flies that were raised axenically to be able to distinguish if the JAK/STAT response is a result of the irradiation damage or loss of bacterial presence. Additionally, the effects of irradiation on superoxide presence were also assessed using DHE dye. A final question explored was whether the reverse is possible: that there is clock dependence on the JAK/STAT pathway. This was accomplished by creating a *Drosophila* strain that overexpressed the unpaired cytokine in a clock reporter background.

CHAPTER 2:

METHODS OF INVESTIGATION

2.1 Drosophila Genetics

Most assays used control (; $\frac{\text{6XSTAT−dGFP}}{+}$;) female flies, and circadian clock mutant (per^{01}; $\frac{\text{6XSTAT−dGFP}}{\text{Cyo}}$;) female flies, unless otherwise noted. These strains contain a heterozygous copy of the 6XSTAT-dGFP reporter. To obtain this in the control strains, the STAT reporter strain (; 6XSTAT-dGFP ;) was crossed with a balancer strain (; w^{1118} ;) to obtain a heterozygous copy of the STAT reporter (; $\frac{\text{6XSTAT−dGFP}}{+}$;). The clock mutant strain stock already contained flies with the heterozygous copy of the STAT reporter (it was not able to homozygose in the mutant background), and the balancers were checked to ensure the heterozygous (; $\frac{\text{6XSTAT−dGFP}}{+}$;) flies were selected.

To obtain the desired amount of eggs for the axenic assay, flies were amplified in bottles until 200 female virgin flies were collected of each required genotype. This ensured that the crosses could be set up using large embryo collection cages (FlyStuff, cat. no. 59-101). The desired progeny of the crosses included a control strain with a heterozygous STAT reporter copy (; $\frac{\text{6XSTAT−dGFP}}{+}$;) and a clock mutant strain with a heterozygous STAT reporter copy (per^{01}; $\frac{\text{6XSTAT−dGFP}}{\text{Cyo}}$;). Apple juice agar (consisting of 61% dH_2O, 29% apple juice, 4% of 95% ethanol, 3% sugar and 3% agar) was set in 100 x 15mm petri dishes (Thermo Scientific, cat. no. 12600002). The apple juice agar plates were then placed at the bottom of the embryo collection cage for egg collection. To encourage egg laying, a 5% yeast paste (consisting of dry yeast and tap water) was spread over top of the apple juice agar. The flies to be crossed were combined in the embryo collection cage for mating at 7:00a.m. and removed at 7:00p.m., for a total mating

period of twelve hours. After mating, the petri dish containing the apple juice agar was removed and the embryos were collected using a paintbrush.

In order to obtain the required genotype for the clock dependence assay in *Section 2.8 Clock Dependence on the Drosophila JAK/STAT Pathway*, a cross between the myo1A-GAL4 enterocyte-specific temperature sensitive strain (; $\frac{\text{myo1A}-\text{Gal4}}{\text{Cyo}}$; $\frac{\text{tub}-\text{Gal80}^{\text{ts}}}{\text{TM6B}}$) and the UPD overexpression strain, which also contain the $\text{Clock}^{\text{PER}}$ reporter, (; $\frac{\text{UAS}-\text{UPD}}{\text{Cyo}}$; $\frac{\text{Clock}^{\text{PER}}}{\text{TM6B}}$) was set up to obtain the resulting genotype, (; $\frac{\text{myo1A}-\text{Gal4}}{\text{UAS}-\text{UPD}}$; $\frac{\text{tub}-\text{Gal80}^{\text{ts}}}{\text{Clock}^{\text{PER}}}$). Similarly, a cross was set-up to obtain a heterozygous control with a $\text{Clock}^{\text{PER}}$ reporter copy. The myo1A-GAL4 temperature sensitive strain (; $\frac{\text{myo1A}-\text{Gal4}}{\text{Cyo}}$; $\frac{\text{tub}-\text{Gal80}^{\text{ts}}}{\text{TM6B}}$) was crossed with the $\text{Clock}^{\text{PER}}$ reporter strain (; $\frac{+}{+}$; $\frac{\text{Clock}^{\text{PER}}}{\text{Clock}^{\text{PER}}}$) to obtain the heterozygous $\text{Clock}^{\text{PER}}$ reporter strain (; $\frac{\text{myo1A}-\text{Gal4}}{+}$; $\frac{\text{tub}-\text{Gal80}^{\text{ts}}}{\text{Clock}^{\text{PER}}}$), which acted as the experimental control.

2.2 Drosophila Maintenance and Circadian Assays

2.2A Standard Rearing and Synchronization

Flies were raised in *Drosophila* polypropylene vials (Fisherbrand Narrow Diameter Vials, 3.74 inches x 0.98 inches, cat. no. AS-507) containing 65% cornmeal, 15% dry yeast, 10% soy flour, 5% malt and 5% agar and were flipped onto new food every second day. The female flies were raised in an LD photoperiod (12 hours light:12 hours of dark, where ZT0 = 7:00 a.m.) in a 25°C incubator (VWR) for at least five days to allow for synchronization. For experiments, the flies were aged between seven to eleven days old unless otherwise noted. To test free

running conditions, the flies were shifted to DD (continuous dark) conditions, in the 25^{o}C incubator, 24-hours before the experiment. To handle flies that are under DD conditions, a red light was used because it has a peak absorbance of 700nm (Baik *et al.*, PNAS, 2019). CRY, the protein that detects light to entrain the circadian clock, has two peak absorbances: 365nm (ultraviolet light) and 450nm (blue light) (Baik *et al.*, PNAS, 2019), thus the red light will not activate the CRY protein and affect the circadian clock. All other light sources were covered. This is critical, as a pulse of light can reset the clock. The shift from LD to DD conditions results in a notation change from ZT to Circadian Time (CT). ZT is a 24-hour notation with ZT0 noting the beginning of the light phase and ZT12 noting the beginning of the dark phase. In comparison, CT time is representative of free running conditions, so CT0 notes the beginning of the subjective day and CT12 notes the beginning of the subjective night.

2.2B Intestinal Dissections and Staining (DAPI and DHE)

All intestinal dissections were performed at room temperature under a stereoscope (Zeiss, Stemi 2000). The flies were anesthetized using carbon dioxide and then sacrificed in a nine well Pyrex spot plate (Thermo Fisher, cat. no. 13-748B) in wells containing 70% ethanol for two minutes. The flies were then transferred to wells containing cold 1 x phosphate buffer saline (1 x PBS at a pH of 7.4) [1mM sodium phosphate dibasic (Sigma Aldrich, cat. no. P332), 0.18mM potassium phosphate monobasic, (Sigma Aldrich, cat. no. P8709) and 15.5mM sodium chloride (Sigma Aldrich, cat. no. S271)]. Then, the flies were dissected using Dumont Inox #5 fine forceps (Fine Science Tools, cat. no. 11251-10). The intestines were fixed using cold 4% paraformaldehyde (PFA) (Electron Microscopy Sciences, cat. no. 15714-5), in PBS for forty minutes. The intestines were rinsed in cold PBS and then stained with 4',6-diamidino-2-

phenylindole (DAPI, 5mg/mL) (Thermo Fisher, cat. no. D1306) in 0.2% PBS-T [TritonX100 (Fisher Scientific, cat. no. BP151), and 1 x PBS] with a pH of 7.4 for five minutes. Following that, the intestines were then rinsed with PBS-T and subjected to two washes of PBS-T for five minutes per wash. The intestines were then ready to be mounted on a glass slide using a droplet of Prolong Gold antifade mountant (Invitrogen, cat. no. P36935). Once the slide had dried after a few days, the cover slip edges were sealed using clear nail polish.

The protocol for using DHE dye outlined by Owusu-Ansah & colleagues (Protec Exch, 2008) was adapted and optimized to detect reactive oxygen species (ROS) in *Drosophila* intestines. On the day of the experiment, the flies were exposed to irradiation set to 15Gy. For dissections, flies were not anaesthetized, as this could interfere with the production of ROS. Instead, flies were tapped to the bottom of the fly vial and transferred to a nine well Pyrex spot plate containing room temperature Schneider's *Drosophila* media supplemented with L-glutamine and sodium bicarbonate (Gibco, cat. no. 21720024). A 30mM stock solution of DHE (Invitrogen, cat. no. D11347) in anhydrous dimethyl sulfoxide (DMSO) > 99.9% (Sigma Aldrich, cat. no. 67-68-5) was prepared immediately before use. From this stock solution, a 30µM final dye concentration was made using the reconstituted DHE and DMSO solution along with room temperature Schneider's media. This final DHE stock solution is light sensitive, so from this point onwards, all incubations were done in the dark using a piece of standard aluminum foil to cover the Pyrex spot plate. The intestines were then incubated with the DHE final stock solution, in the dark, on an orbital shaker (Fisher Scientific) for seven minutes. The intestines were then subjected to three five-minute washes in room temperature Schneider's media while maintaining the dark conditions. Next, a mild fixation was performed. Intestines were fixed in room temperature 4% PFA for seven minutes in the dark. After fixation, the

intestines were rinsed in room temperature 1 x PBS and stained with room temperature DAPI for five minutes in the dark. The intestines were then subjected to a 0.2% PBS-T rinse at room temperature and subsequently underwent two five-minute 0.2% PBS-T washes at room temperature in the dark. The intestines were then mounted on a glass slide using Prolong Gold antifade mountant, taking caution to keep the intestines protected from the light. After approximately six hours, the cover slip edges were sealed using clear nail polish.

2.3 JAK/STAT and Circadian Clock Reporters

To visualize STAT activity *in vivo*, a 6XSTAT-dGFP reporter was obtained (He *et al.*, eLife, 2019). Prior to experimentation, reporter activity was tested using three different treatments: 5g of Dextran Sulfate Sodium (DSS) (MP Biomedicals, cat. no. 160110) in 100mL of sucrose, 25µg/mL of Bleomycin and 5mg/mL of sucrose in tap water through a 48-hour treatment administration. DSS and Bleomycin solutions were the positive control treatments and the sucrose solution was used as a negative control treatment. The STAT reporter function was confirmed by cross-referencing previous work by Buchon and colleagues (Cell Reports, 2013) that found JAK/STAT activity is present in enteroblasts and intestinal stem cells (Parasram, unpublished).

2.4 X-Ray Irradiation Assay

2.4A Survival Assay

Irradiation was performed at four different times of day (7p.m., 1p.m., 7p.m., and 1a.m.). Eight groups of 25 female control flies were collected upon eclosion. The flies were raised in a

25°C incubator under LD conditions (7:00a.m. lights on, ZT0, and 7p.m. lights off, ZT12) from eclosion until their death. For each time point, there was an undamaged group, which did not receive any irradiation damage. X-ray irradiation was administered using the Faxitron X-ray System (Model #43855D, Option #RX-650) set at 15Gy. Immediately following irradiation, the flies were flipped to a vial containing fresh food, then flipped to fresh vials every other day. The number of deaths were scored daily.

2.4B JAK/STAT

Groups of 12 to 15 female control flies were raised in a 25°C incubator oscillating in a LD cycle, where lights turned on at 7:00a.m. (ZT0) and lights turned off at 7:00p.m. (ZT12). The flies were flipped to new vials every other day. At seven days old, the flies were irradiated at ZT0 (7:00a.m.) in an x-ray irradiator set to 15Gy. Following irradiation, the flies were dissected at six different time points: one-hour post irradiation (ZT1), two-hours post irradiation (ZT2), three-hours post irradiation (ZT3), four-hours post irradiation (ZT4), five-hours post irradiation (ZT5) and six-hours post irradiation (ZT6).

2.4C Smurf Assay

A sample size of 18 control female flies were raised in a 25°C incubator, where the lights turned on at 7:00a.m. (ZT0) and turned off at 7:00p.m. (ZT12). They were flipped to fresh food every three days. 24-hours prior to x-ray irradiation exposure, the flies were fed a 2.5% Bromophenol blue solution [250mg Bromophenol Blue, (Fisher Scientific, cat. no. 115-39-9) and 10mL 5% sucrose (Fisher Scientific, cat. no. 55-3)] in tap water using a moistened Whatman filter paper in a *Drosophila* vial. The following day (when the flies were eight days old), they

were exposed to 15Gy of irradiation at ZT0 (7:00a.m.). Immediately following irradiation treatment, the flies were flipped into new vials containing the 2.5% Bromophenol blue solution on a Whatman filter paper. The flies were observed regularly throughout the day (immediately after irradiation, one-hour post irradiation, two-hours post irradiation, three-hours post irradiation, four-hours post irradiation, five-hours post irradiation, nine-hours post irradiation, 12-hours post irradiation and 24-hours post irradiation) to classify each flies' degree of 'smurfness' over the course of 24 hours.

2.4D X-Ray Irradiation and Nuclear Morphology

On experiment day, control flies were transported to the irradiation room and maintained in dark conditions using a 50mL conical tube (Thermo Scientific, cat. no. 339653) wrapped in standard aluminum foil, such that no light could penetrate through the tube. Once the irradiation room was reached, the lights remained off. Experimental flies were subjected to x-ray irradiation of 15Gy using the Faxitron X-ray System. Four different time points within a 24-hour period were chosen for irradiation: circadian time (CT) 24 (7:00a.m.), CT30 (1:00p.m.), CT36 (7:00p.m.) or CT42 (1:00a.m). Following irradiation, the flies were put back in the DD incubator, until it was time to be dissected three-hours post the time of irradiation.

To observe the effects of acute damage on the *Drosophila* intestine using different reporters related to stress, a JNK reporter strain (; JNK-dGFP ;) and a Hippo reporter strain (; YKI-dGFP:RFP ;) were tested for reporter function in the intestine. Flies were exposed to a 48-hour treatment of a negative control (5% sucrose) or a treatment group consisting of a chemical (2% H_2O_2 or bleomycin) in 5% sucrose (Figure 8). Following the corresponding treatments, the flies were dissected and scanned using a slide scanner. The JNK reporter (; JNK:dGFP ;) was

tested first. The negative control (expected to have low JNK activity) had very little to no GFP+ cells present, while the treatment groups (expected to have high JNK activity) had GFP+ cells present, but the fluorescence intensity was low. The negative control and treatment groups of the Hippo reporter strain (; YKI-dGFP:RFP ;) were tested, but no signal was detected, so it was not used in any other assays.

FIGURE 8

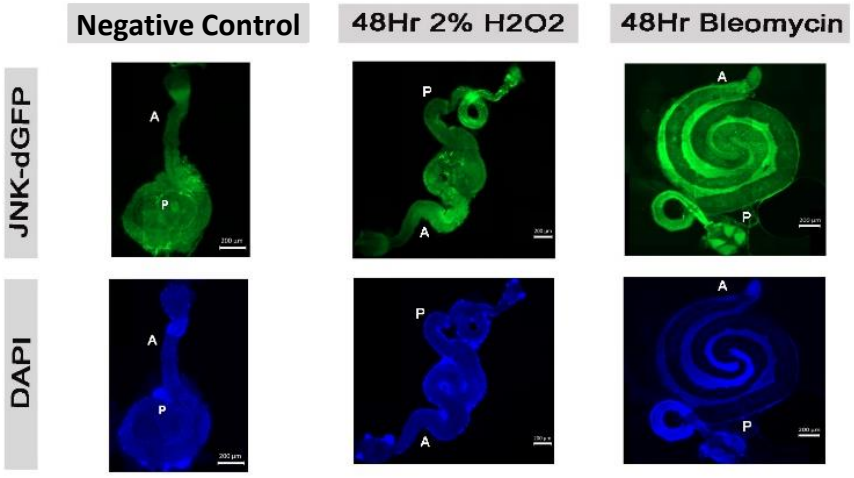

Figure 8: JNK Reporter Verification
Representative slide scanner images of positive and negative controls used to verify JNK reporter activity. It is evident that there is little JNK reporter activity (GFP+ cells) present in the negative control (5% sucrose). The positive treatment groups consist of the chemical (2% H_2O_2 or bleomycin) + 5% sucrose. In the positive controls, some JNK reporter activity present, particularly in the anterior region. 'A' indicates the anterior portion of the intestine and 'P' indicates the posterior portion of the intestine, scale bar represents 200µm.

A sample size of 55 JNK reporter flies were collected and synchronized in a 25°C incubator on a LD cycle, where the lights turned on at 7:00a.m. (ZT0) and the lights turned off at 7:00p.m. The flies were flipped onto fresh food every other day. At six to seven days old, the flies were irradiated at ZT0 (7:00a.m.) in an irradiator set to 15Gy and following irradiation, the

flies were flipped into fresh vials. The flies were dissected at various times of day post irradiation [8:00a.m. (ZT1), 9:00a.m. (ZT2), 10:00a.m. (ZT3), 11:00a.m. (ZT4), 12:00p.m. (ZT5), 1:00p.m. (ZT6), 4:00p.m. (ZT9), 7:00p.m. (ZT12), 1:00a.m. (ZT18) and 7:00a.m. the following day (ZT24)].

2.5 Axenic Assay

New *Drosophila* 25mm glass vials (Fisher Scientific, cat. no. AS574) and a cotton ball were wrapped together in standard aluminum foil. Prior to usage, the pair was autoclaved at 121^{o}C for 45 minutes. The vials were filled with standard *Drosophila* food supplemented with four broad spectrum antibiotics adapted from Iatsenko and colleagues (Immunity, 2018). This antibiotic cocktail consisted of: carbencillin sodium salt (Fisher Scientific, cat. no. BP2648) in dH_2O at 50µg/mL, kanamycin sulfate (Fisher Scientific, cat. no. AC611290050) in dH_2O at 50µg/mL, tetracyclin (Sigma Aldrich, cat. no. 87128) in dH_2O at 10µg/mL and erythromycin (Sigma Aldrich, cat. no. E5389) in dH_2O at 10µg/mL. The vials were set aside until the embryo collection step.

To maintain axenic conditions, the collected embryos from the apple juice agar plates were put into a 100µm cell strainer (Fisher Scientific, cat. no. 352360) and subsequently underwent a bleaching wash using a 7% bleach solution. The embryos were rinsed with water and the 7% bleach wash was repeated. Next, the embryos underwent three successive washes using a *Drosophila* embryo wash. A paintbrush was used to transfer the bleached embryos from the cell strainer to the *Drosophila* vial containing the food supplemented with the antibiotic cocktail. The embryo-containing vials were then placed in a 25^{o}C LD incubator until eclosion.

Upon eclosion, 15 female flies with the desired genotype and sex were identified and placed into new vials containing the food supplemented with the antibiotic cocktail. The flies were flipped onto fresh food every second day. The flies were raised and synchronized in a 25°C incubator on a LD cycle, where ZT0 was at 7:00a.m. 24-hours prior to irradiation, the flies were shifted to DD conditions. On the day of the experiment, the flies were aged between eight to eleven days old and irradiated with 15Gy at CT30 (1:00p.m.) or CT42 (1:00a.m.). Immediately after irradiation, the flies were flipped into fresh vials and were stored in the 25°C incubator until it was time for the dissection, three hours post irradiation.

2.6 Microscopy and Slide Imaging

A Zeis Axio Vert A.1 inverted fluorescence contrast microscope, with GFP and DAPI channels, was preliminary used to observe qualitative differences in staining. To obtain representative images and to analyze the images, a Zeiss Axio Scan Z.1 slide scanner was used. A scanning profile that incorporated GFP and DAPI channels was selected for imaging (and the QD605 channel for DHE, when necessary). For the DHE stained slides, imaging was performed as soon as possible to prevent DHE fluorescent signal degradation.

2.7 Image Analysis and Statistics

2.7A X-Ray Irradiation Image Analysis

The slide scanner images were quantified using the Zen Blue Axio Scan Z.1 software (Zeiss). The fluorescence levels of GFP/DHE and DAPI staining were quantified. All of the GFP/DHE positive cells within the region of interest were circled allowing the Axio Scan

software to provide a corresponding fluorescence intensity for each circled cell. The total number of DAPI+ cells within this region were manually counted using a hand-held tally counter. The levels of GFP/DHE positive cells were normalized to DAPI because each treatment had the same exposure time and the same concentration to the DAPI stain, so it should be consistent across each sample. This data was entered into Microsoft Excel, using a threshold intensity of 2000 for GFP+ cells and no threshold intensity for DHE+ cells. The number of cells reaching this threshold were recorded for each time point. These values were organized into a spreadsheet in Microsoft Excel and an average ratio of GFP/DHE positive cells to DAPI+ cells was determined. This data was then graphed into Prism 7 software (Graphpad), where the appropriate statistics were performed. Statistical significance is noted as p values, where values less than 0.05 were considered statistically significant.

For the clock dependence on the JAK/STAT assays, the fluorescence intensity of each sample was achieved by using the Zen Blue Axio Scan Z.1 software. For each sample, the whole intestinal region (R1 to R5), the anterior portion of the intestinal region (R1), the mid-intestinal region (R2, R3 and R4) and the posterior portion of the intestinal region (R5) were examined separately. Using the Spline tools in the Zen Blue Axio Scan Z.1 software program, the desired area of interest was outlined. Once outlined, the program provided an overall fluorescence value for each of the scanned channels (GFP and DAPI). These values were inputted into a Microsoft Excel spreadsheet and an average ratio of GFP fluorescence intensity to DAPI fluorescence intensity was determined for each treatment group and time point. These values were graphed using Prism Software (Graphpad) and appropriate statistics were performed using the Prism software, and statistical significances are expressed as p values.

2.7B Nuclear Morphology Image Analysis

Using the Zen Blue Axio Scan Z.1 software, a preset rectangle with an area of 8730μm^2 was randomly positioned within the inner portion of the R5 intestinal region. The GFP+ cells within this region were circled and the total number of DAPI+ nuclei within this region were counted using a tally counter. Any positive nuclei touching the border of the preset area were considered. Data output on the scanning software provided the area of each circled unit, which was used as a representative measure of cell size. The data was organized into Microsoft Excel and using Prism software, representative graphs summarizing the total number of nuclei, the average nuclear size and the breakdown of larger nuclei (nuclear area > 5μm^2) versus smaller nuclei (nuclear area ≤ 5μm^2) were constructed. Appropriate statistics were performed using Prism software, and significance is expressed as p values.

2.8 Clock Dependence on the Drosophila JAK/STAT Pathway

16 groups of six to ten flies containing the UAS/GAL4 gene expression system were collected, allowing for regional and temporal control of UPD overexpression. Upon eclosion, the flies were raised and synchronized in a 29^oC incubator on a LD cycle, where 7:00a.m. lights turned on (ZT0) and at 7:00p.m. the lights turned off (ZT12). At five days old, the flies were dissected at eight different time points over a 24-hour period: 7:00a.m. (ZT0), 10:00a.m. (ZT3), 1:00p.m. (ZT6), 4:00p.m. (ZT9), 7:00p.m. (ZT12), 10:00p.m. (ZT15), 1:00a.m. (ZT18) and 4:00a.m. (ZT21).

CHAPTER 3

RESULTS

3.1 Effects of Irradiation Damage

To be able to test circadian regulation of damage timing in the *Drosophila* intestine, an acute damage assay was developed. This was important, because the time of the damage had to be much shorter than 24 hours, and ideally had to be rapid so that differences between times of day could be tested. Various methods of acute damage induction to the *Drosophila* intestine were explored. One of the first methods explored was physical damage. A 'clam-shell' approach dissection was performed to expose the intestine but keep it housed within the abdomen (Figure 9). The R5 region of the abdomen was pinched using fine forceps and left in the PBS until it was time for the intestinal dissection. Intestines were dissected at one-hour post pinching, 12-hours post pinching, 24-hours post pinching and 48-hours post pinching. By the 12-hours post pinching dissection, the intestine started to break down and become extremely brittle to handle. To slow down the intestinal degradation, Schneider's Insect Media (commonly used for insect cell cultures) could be used. Another limitation to this method is that it is difficult to reproduce. The force of pinching exerted and location chosen to pinch is all relative to the experimenter. This method was not reproducible enough to proceed.

FIGURE 9

Figure 9: 'Clam Shell' Dissection for Pinching Assay
Example of a 'clam shell' dissection of the *Drosophila* abdomen to expose the intestine for the pinching assay. Image taken from a stereoscope at 25x magnification.

Another type of damage tested was acute chemical damage. The flies were fed bleomycin solutions or 5% DSS solutions for a short period of time (48-hours) prior to experimentation. Bleomycin is an anti-cancer drug that has been used in experimentation as a DNA damaging agent (Takada *et al*., Cell, 2003) that specifically damages enterocytes (Amcheslavsky *et al.*, Cell Stem Cell, 2009). DSS is another damaging agent that causes extreme intestinal inflammation that resembles ulcerative colitis (Amcheslavsky *et al.*, Cell Stem Cell, 2009). A limitation is that it cannot be ensured that each animal will ingest these damaging agents so the degree of damage could vary. To minimize this possibility, the flies are often starved prior to exposure to the damaging agent. These treatments were ultimately used as the positive controls for JAK/STAT activity because they have been shown to promote cellular proliferation. However, the timing of the bleomycin ingestion took hours and thus I did not continue with this method.

The third type of damage tested was through x-ray irradiation. The robust survivability and resilience of *Drosophila* larvae against irradiation damage has been previously tested.

Verghese and Su (PLoS Biol, 2016) tested this robustness and exposed *Drosophila* larvae to a maximum of 80Gy of irradiation. The damaging effect of irradiation killed at least half of the cells in the imaginal discs but despite that damage, the flies maintained normal features and a normal longevity (Verghese and Su, PLoS Biol, 2016). I attempted a much lower dose. The flies were exposed to a peak kilovoltage of 75 for seven and a half minutes set to 15Gy and since they were able to survive the exposure, this was the irradiation dosage chosen for this assay. Irradiation was the most acute and reproducible and reliable form of acute damage of the three methods attempted.

To obtain more consistent results with the STAT reporter, various factors were tested and controlled when designing this assay. These factors include: movement effects, bottle care, smell effects, dissection/ fly handling technique, length of dissection, age of experimental flies and using a homozygous reporter copy versus a heterozygous reporter copy. As an additional precaution to ensure the fly stocks were not contaminated, new fly stocks were obtained and raised prior to performing the experiment. The fly stock vials were also flipped onto different batches of fly food, preemptively, as a precaution if a batch of food was unknowingly contaminated. Table #1 highlights the various troubleshooting efforts and the result of implementing each change.

Table #1 Irradiation Assay Troubleshooting

Troubleshooting Topic	Description	Result
Movement Effects	To transport experimental flies, a Styrofoam transport box was placed inside a cardboard box, in attempt to stabilize the vials and reduce the movements associated with walking between the incubator room to the irradiator room (see set-up in Figure 10).	No change
Smell Effects	A previous study by Brenman-Suttner and colleagues (Scientific Reports, 2018) suggests that odorants could cause a stress response in flies. To control for this, it was ensured that no perfume or fragrances were worn while handling the flies. This study also suggested that when flies are overcrowded, they can emit stress odorants so it was ensured that the flies being raised had adequate social distance to prevent the emission of stress odorants and no more than 20 flies (15 females and 5 males) were raised in each vial.	Reporter activity was more consistent when taking into account social distancing.
Bottle Care	To enhance bottle care handling, experimental flies were flipped onto fresh food every other day. Additionally, no more than 20 flies were raised in each vial, as mentioned above.	Reporter activity was more consistent
Dissection/ Fly Handling Technique	Prior to experimenting, approximately 200 fly dissections were performed to ensure consistency. Different intestinal dissection techniques were carried out to determine if dissection technique had an effect on reporter activity.	No change
Dissection Length	There is a 1.5-hour maximum time limit beginning from the time the anesthetized flies are put in the 75% ethanol to the time the dissected intestines (in PBS) are fixated in 4% PFA. This is to ensure that the time points do not overlap with one another. Dissections were performed in one hour or less to ensure the time intestines spent in PBS was not a factor.	No change
Age of Experimental Flies	When performing intestinal dissections, flies should be between five to 14 days old. The intestine is not fully developed until five days of age and any flies older than 14 days are too old for experimentation.	No change
Reporter Copy	The strain of flies could contain a heterozygous or homozygous copy of the reporter. The homozygous copy had a strong signal and was not very consistent. Instead, the heterozygous copy was used as it yielded more consistent results with an appropriate reporter signal strength.	Reporter activity was more consistent

FIGURE 10

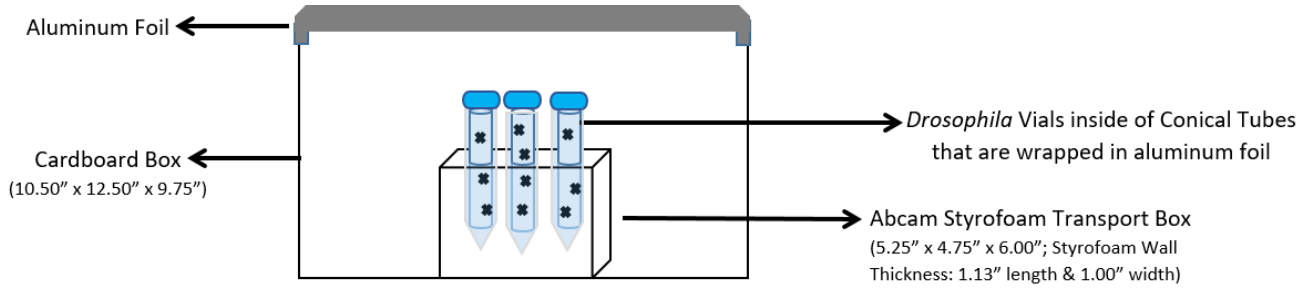

Figure 10: Transportation Set-Up to Minimize Movement Effects
Diagram depicting the set-up when transporting flies from the incubator room to the x-ray irradiator room. This set-up was designed to maintain dark conditions preventing any light from penetrating through to the flies.

Overall, it was a combination of the various troubleshooting topics that were incorporated into the development of the x-ray irradiation assay to be able to yield the most consistent results.

3.1A Drosophila Survival

The original plan was to start by administering a high dosage of irradiation (a peak kilovoltage of 75 in order to achieve a peak of 15Gy) and observe if the flies will survive or die from the irradiation exposure. If the flies had died, then a lower dose of irradiation would have been tested. To observe the effects of irradiation on the survivability of *Drosophila*, a control (; 6XSTAT-dGFP ;) group and a period mutant group (per^{01}; $\frac{6XSTAT-dGFP}{Cyo}$;) were raised in LD conditions and tested. Additionally, to determine if the timing of damage affects survival, each group was irradiated at different times throughout the day, ZT0 (7:00a.m.), ZT6 (1:00p.m.), ZT12 (7:00p.m.) or ZT24 (1:00a.m.).

It was determined that the dosage and timing of 15 gray irradiation exposure did not affect the long-term survival of the control flies or period mutant flies as seen in Figure 10. The

y-axis indicates the percent survival of flies, where a value of 100 on the y-axis implies that all the flies are alive. The control flies had the longest lifespan (approximately 100 days old) and the period mutant flies had a shorter lifespan (approximately 70 days old). This observation supports the findings by Klarsfeld & Rouyer (J Biol Rhythms, 1998) which found that period mutant flies have a shorter lifespan than the control strain. Recently, Ulgherait and colleagues (Nat Commun, 2020) found that period mutant *Drosophila* strains have a longer lifespan than the control strain, but this is inconsistent with both my data and the previously published findings. Kaplan Meier survival statistics were significant across all the various times of irradiation (Figures 11 A - E). When comparing each strain across each time of irradiation (Figure 11 F – G), it is evident that the control has differences based on the time of irradiation whereas these differences are not observed in the period clock mutant. The control flies irradiated at ZT0 have a lower survival at day 50 (Figure 11B) in comparison to the control flies irradiated at the other times of day. Surprisingly, this reduction in survival at day 50 does not affect the overall long-term survival of the surviving flies.

FIGURE 11

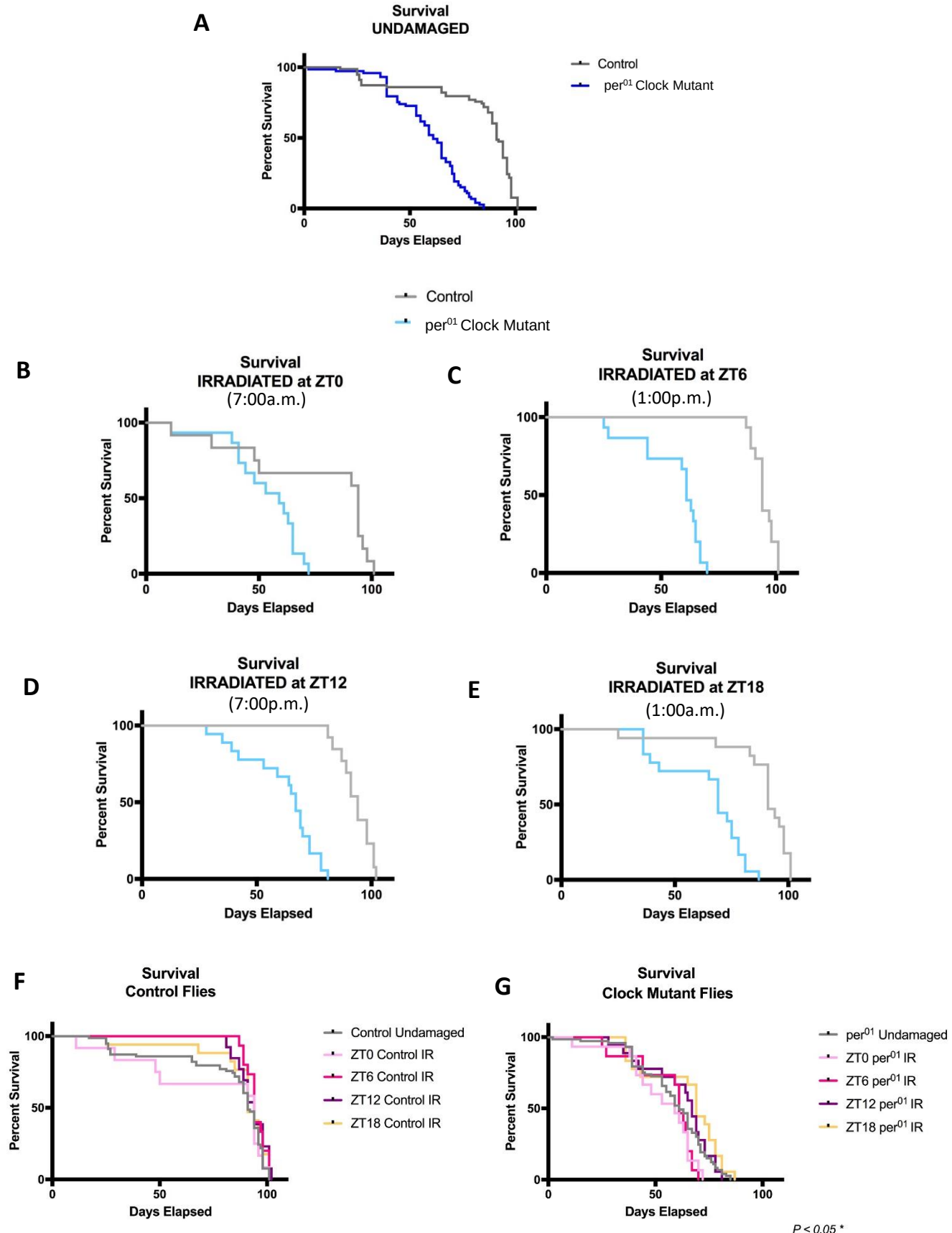
A
Survival
UNDAMAGED
Percent Survival
Days Elapsed
Control
per01 Clock Mutant
B
Survival
IRRADIATED at ZT0
(7:00a.m.)
C
Survival
IRRADIATED at ZT6
(1:00p.m.)
D
Survival
IRRADIATED at ZT12
(7:00p.m.)
E
Survival
IRRADIATED at ZT18
(1:00a.m.)
F
Survival
Control Flies
Control Undamaged
ZT0 Control IR
ZT6 Control IR
ZT12 Control IR
ZT18 Control IR
G
Survival
Clock Mutant Flies
per01 Undamaged
ZT0 per01 IR
ZT6 per01 IR
ZT12 per01 IR
ZT18 per01 IR
P < 0.05 *

Figure 11: Kaplan Meier Survival Curves for Control and Period Clock Mutant Flies Under Undamaged Conditions or Exposed to 15Gy Irradiation at Various Times of Day.
The control flies irradiated at ZT0 have a decreased lifespan between days 11 to 90 in comparison to control flies irradiated at other times of day. There are differences in control survival based on time of irradiation (Fig. 11F), which is not seen in the period clock mutant (Fig. 11G).
(A) Survival curve for undamaged flies. Data presented for undamaged n= 84 control flies and n= 63 clock mutant flies [Mantel-Cox Log Rank Test, Chi Square= 90.74, df= 1, $p < 0.0001$ (****)].
(B) Survival curve for flies irradiated at ZT0 (7:00a.m.). Data presented for n= 16 control flies and 15 clock mutant flies Mantel-Cox Log Rank Test, Chi Square= 9.05, df= 1, p= 0.0026 (**)].
(C) Survival curve for flies irradiated at ZT6 (1:00p.m.). Data presented for n= 19 control flies and 15 clock mutant flies [Mantel-Cox Log Rank Test, Chi Square= 33.34, df= 1, $p < 0.0001$ (****)].
(D) Survival curve for flies irradiated at ZT12 (7:00p.m.). Data presented for n= 21 control flies and n= 17 clock mutant flies [Mantel-Cox Log Rank Test, Chi Square= 29.84, df= 1, $p < 0.0001$ (****)].
(E) Survival curve for flies irradiated at ZT18 (1:00a.m.). Data presented for n= 23 control flies and n= 18 clock mutant flies [Mantel-Cox Log Rank Test, Chi Square= 24.78, df= 1, $p < 0.0001$ (****)].
(F) Survival curve for control flies. Data presented for undamaged n= 84 flies and irradiated n= 16- 22 flies per group [Mantel-Cox Log Rank Test, Chi Square= 5.092, df= 4, p= 0.2780 (*n.s.*)].
(G) Survival curve for period mutant flies. Data presented for undamaged n= 63 flies and irradiated n= 14-18 flies per group [Mantel-Cox Log Rank Test, Chi Square= 12.82, df= 4, p= 0.0122 (*)].

3.1B JAK/STAT Reporter Activity Levels

The activity levels of the JAK/STAT reporter were tested in order to determine whether JAK/STAT activity changes after exposure to acute damage. The *Drosophila* with the control genotype (with a heterozygous copy of the STAT reporter) were raised in LD conditions and were all irradiated at ZT0 (7:00a.m.). Six dissection times post irradiation were performed at one hour intervals, beginning at ZT1 (8:00a.m.) and continuing up until ZT6 (1:00p.m.). The STAT reporter is situated upstream of a dGFP fluorescent tag. Thus, when a cell fluoresces green under GFP-sensitive fluorescence, it is an indication of the presence of STAT reporter activity.

The first step performed was to image the reporter in the midgut, in particular, the R5 region to determine if there were any preliminary differences in the GFP intensity levels and/or quantity of GFP+ cells. The posterior intestine has the greatest levels of proliferative activity (Takashima *et al.*, Nature, 2008), so the R5 region is expected to be a region with the highest levels of JAK/STAT activity, due to its involvement in regeneration. The image panel depicted in Figure 12A shows a representative image from each time point (one-hour control, one-hour post irradiation, two-hours post irradiation, three-hours post irradiation, four-hours post irradiation, five-hours post irradiation and six-hours post irradiation), with the GFP+ cells in green. DAPI was used as a nuclear counterstain to ensure background fluorescent artefacts were not mistaken to be part of a cell. Both the number of GFP+ cells and the fluorescent intensity of the GFP+ cells were considered while observing these samples. It was determined that the samples from three-hours post irradiation and four-hours post irradiation appeared to have the most GFP+ cells, especially when compared to the one-hour control samples that were not irradiated. There are medium levels of GFP+ cells observed at one-hour post irradiation and five-hours post irradiation. Mild levels of GFP+ cells are observed at two-hours post irradiation and six-hours post irradiation. The lowest levels of GFP+ cells are observed in the undamaged one-hour control sample.

To validate these qualitative observations, the intestinal R5 region of these images were subsequently quantified. The total number of GFP+ cells (as a ratio to the total number of DAPI+ nuclei) was determined. Additionally, the GFP intensity level of each GFP+ cell was taken into account. This data was compiled and the graph in Figure 12B was obtained. In corroboration with the observations made in Figure 12A, it was determined that intestinal STAT reporter activity is most active at three-hours post irradiation and four-hours post irradiation

despite all the samples receiving the same dosage and length of irradiation at ZT0 (7:00a.m.). The data distribution is fairly symmetric, in which the highest levels of the STAT reporter are observed at three and four-hours post-irradiation (with a ratio of approximately 0.055 GFP+ cells to total cells). The lowest levels of STAT reporter activity (with a ratio of approximately 0.025 GFP+ cells to total cells) are noted in the undamaged control sample, one-hour post irradiation, two-hours post irradiation and six-hours post irradiation. A medium level of STAT reporter activity was observed at five-hours post irradiation (with a ratio of approximately 0.040 GFP+ cells to total cells). The differences between the levels of STAT reporter activity across the various time points were not significant via a one-way ANOVA. It was ultimately decided to observe the levels of JAK/STAT activity three-hours post irradiation because it was quantified as having one of the highest levels of JAK/STAT activity and it was more convenient when performing 24-hour time series to ensure the time of irradiation did not overlap with the dissection from the previous time point.

FIGURE 12

A

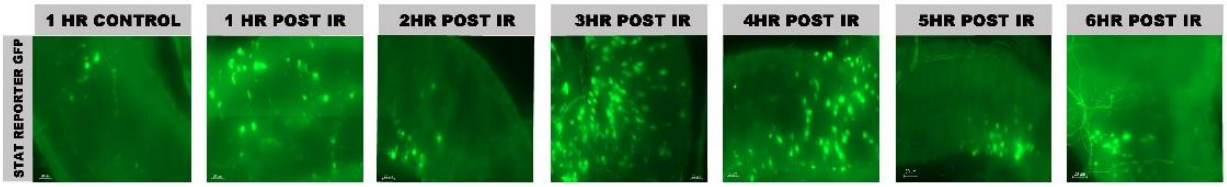

B

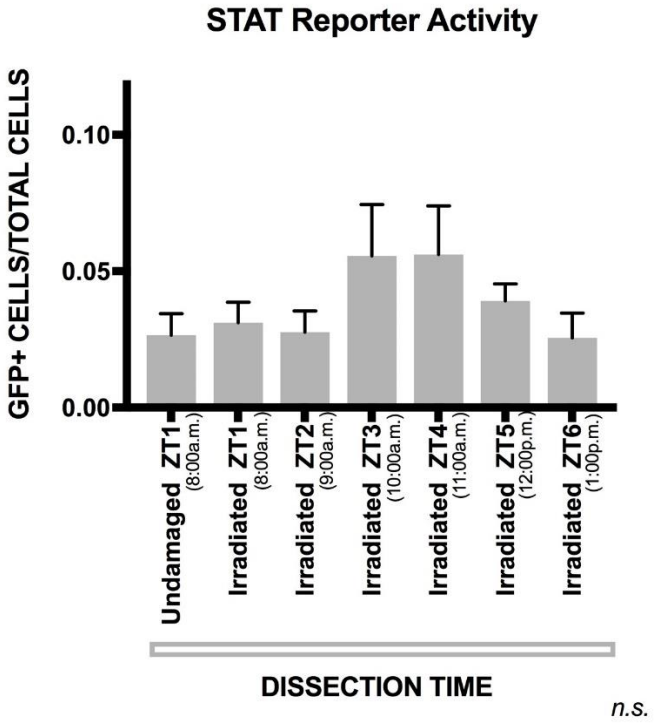

Figure 12: An Optimal Time to Observe Increased Levels of STAT Intestinal Activity is Three Hours, Post-Acute Damage

(A) Representative slide scanner images of the R5 intestinal *Drosophila* region, where GFP+ cells mark STAT reporter activity. Flies were irradiated at ZT0 (7:00a.m.) and then dissected at different times of day post-irradiation. *Drosophila* dissected at three-hours post irradiation have an increased number of STAT positive cells. Scale bar for each image represents 20µm.

(B) Graphical representation of slide scanner images shown in Figure 12A. Flies dissected at three-hours post irradiation and four-hours post irradiation have the greatest ratio of STAT reporter activity. Both the quantity and intensity of GFP-positive cells is incorporated into the

GFP+ cells to total cells ratio. Data presented for n = 8 – 12 intestines in each group, error bars represent + standard error of the mean (SEM). One-way ANOVA, [F = 1.407, p = 0.2259 (*n.s.*)].

3.1C Nuclear Morphology and Nuclear Size

The effects of irradiation on the nuclear morphology of cells in the R5 region of the *Drosophila* intestine were analyzed. The *Drosophila* were raised in LD conditions and then shifted to DD conditions 24-hours prior to the experiment to simulate free-running conditions. The flies were irradiated at one of the four different time points over a 24-hour period (CT24 = 7:00a.m., CT30 = 1:00p.m., CT36 = 7:00p.m., or CT42 = 1:00a.m.) and were later dissected three-hours post-irradiation. DAPI was used as a nuclear counterstain on both undamaged and irradiated intestines (see Figure 13). It was determined that the nuclear morphology of the cells from the undamaged sample were generally larger in size and circular in shape with uniform edges. In comparison, when looking at the damaged sample, there appeared to be an increase in the number of DAPI+ nuclei which consisted of both small and large sized DAPI+ nuclei. Additionally, the edges of the DAPI+ nuclei in the damaged sample were rough and irregular.

FIGURE 13

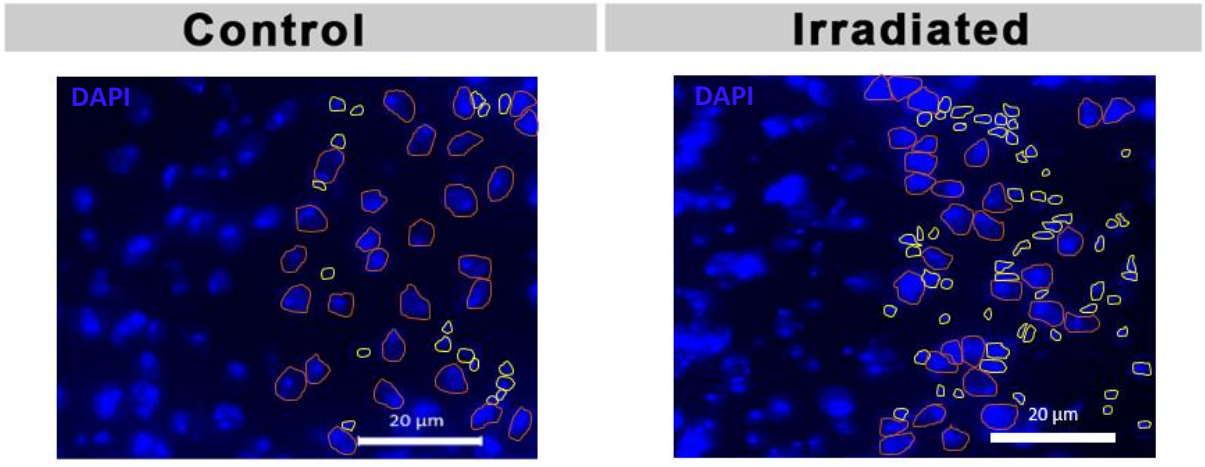

Figure 13: Nuclear Morphology of the *Drosophila* Intestine is Altered After Irradiation
Slide scanner images of a portion of the *Drosophila* R5 region taken from control flies that were acutely damaged via x-ray irradiation at CT42 (1:00a.m.) and subsequently dissected three hours after irradiation. DAPI nuclear staining in an undamaged intestine (left panel) and a damaged intestine (right panel) shows that the nuclear morphology in the damaged intestine appear irregular in morphology and an increase in the number of nuclei present. Representative images were taken on a Slide Scanner with a resolution of 20µm. Examples of large nuclei (with an area greater than 5µm^2) are outlined in orange and examples of small nuclei (with an area less than or equal to 5µm^2) are outlined in yellow on the right hand side of each representative image.

In order to investigate this relationship quantitatively, a preset area was randomly selected within the R5 *Drosophila* region to allow for image analysis.

To determine if there was a significant difference in the average nuclear size between the two treatment groups, average nuclear area was used as a representative measure for average nuclear size. Figure 14A depicts the average nuclear size for each treatment group. The undamaged samples had a significantly larger average nuclear size than the irradiated samples. The average nuclear area for the undamaged samples was approximately 13µm^2 and the average nuclear area for the irradiated group was about half that value, at approximately 7µm^2. When this data is broken down into the various time points of interest (CT24, CT30, CT36 and CT42), it is evident that the trends observed in Figure 14B are consistent with the trends observed in Figure 14A. Across all the time points, Figure 14B illustrates that the undamaged samples have a significantly larger average nuclear size in comparison to the irradiated samples. Furthermore, when comparing a treatment group across each time point, the average nuclear size remained within a close range of values. The average nuclear size for the undamaged treatment group ranged between 12µm^2 and 14µm^2, for CT42 and CT24, respectively. In comparison, the

average nuclear size for the irradiated treatment group ranged between 5μm^2 to 8μm^2, for CT36 and CT24/CT42, respectively.

Next, the scanned images were further quantified to determine the total number of nuclei present within the R5 region preset area previously described. The number of nuclei present was used as a representative sample for the total number of cells present. Figure 14C illustrates the number of nuclei in the undamaged treatment group and the irradiated treatment group. The irradiated treatment group had a significantly greater number of nuclei, with approximately 173 nuclei, whereas the undamaged treatment group had approximately 109 nuclei. This data was also broken down into four corresponding time points: CT24 (7:00a.m.), CT30 (1:00p.m.), CT36 (7:00p.m.) or CT42 (1:00a.m.), over a 24-hour period, to determine if there was any variation in the number of nuclei present at each time point. In accordance with Figure 13C, the irradiated treatment group consistently had a larger number of nuclei present across each time point in comparison to the undamaged treatment group. This suggests that there could be a difference in the number of nuclei present between the control and irradiated treatment groups. It is important to note that there does not appear to be any time of day irradiation differences in the number of nuclei present.

To gain a better understanding of these trends, nuclear area quantifications were separated into two categories: percentage of cells with a nuclear area greater than 5μm^2 (representative of larger nuclei) or percentage of cells with a nuclear area less than or equal to 5μm^2 (representative of smaller nuclei) for each treatment group. The same R5 region preset area described above for quantifying the nuclear size was used. Figure 14E shows that the percentage of larger cells with a nuclear area greater than 5μm^2 is 84.4% for the undamaged group and 51.4% for the irradiated treatment group. This indicates that the presence of larger

nuclei is increased in undamaged intestines in comparison to irradiated intestines. Moreover, it is evident in Figure 14F that the percentage of smaller cells with a nuclear area less than or equal to 5μm^2, have a significant difference between the undamaged and irradiated groups. The undamaged group has a significantly less percentage of nuclei that are smaller in size (averaging approximately 15.6% of cells within the preset area), whereas the irradiated group contains a larger percentage of nuclei that are smaller in size (averaging approximately 48.6% of cells within the preset area). By comparing Figure 14E with Figure 14F, it can be inferred that the average nuclear area in the undamaged treatment group mostly consists of larger nuclei and some smaller nuclei and the irradiated treatment group has increased numbers of smaller nuclei (in comparison to the undamaged sample).

FIGURE 14

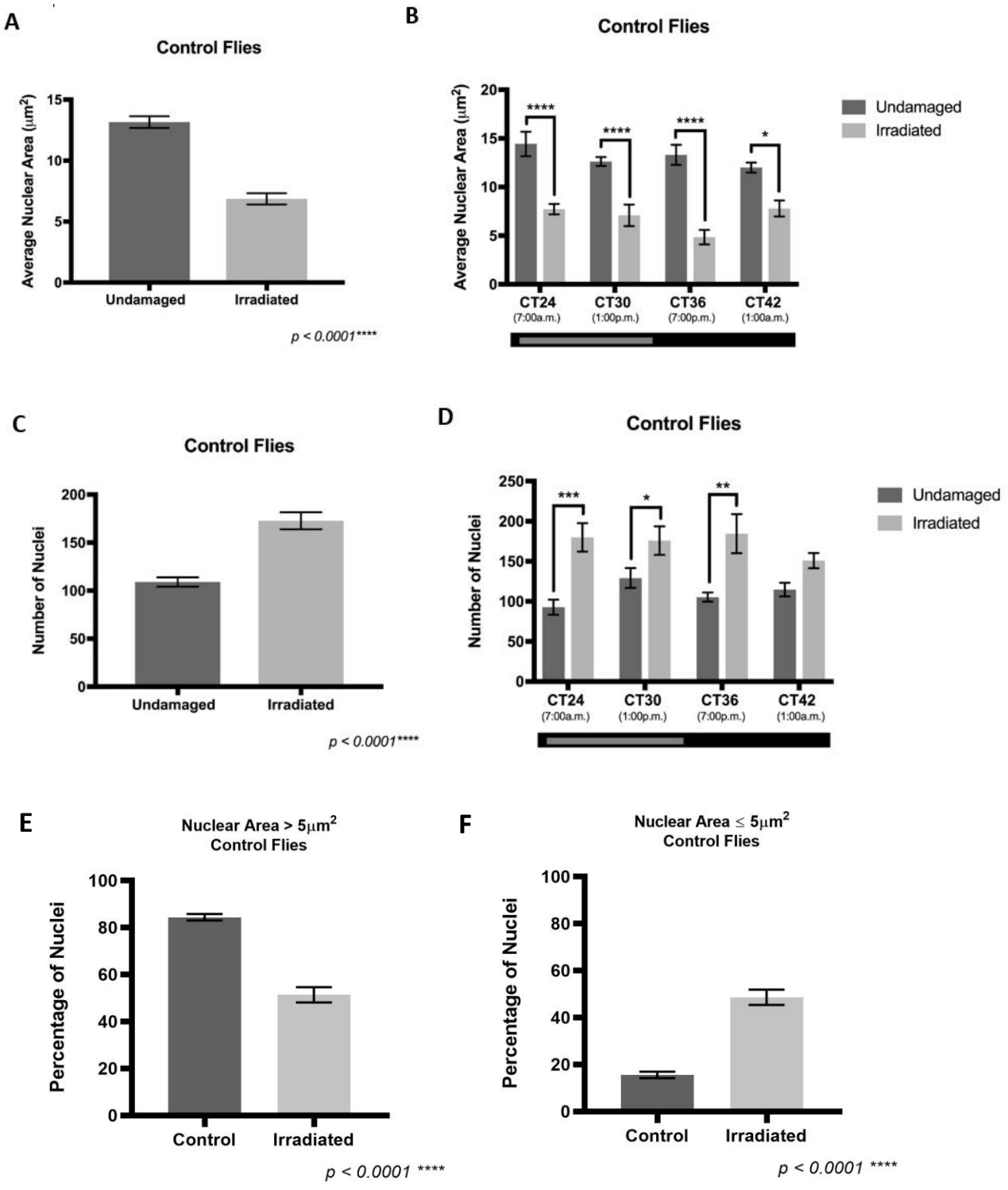

Figure 14: Irradiated Intestines Have More Nuclei That Are Smaller in Size in Comparison to Undamaged Intestines

(A) Analysis of an area within the R5 region from Slide Scanner images of *Drosophila* under free-running conditions, where DAPI staining was indicative of nuclei present. Irradiated intestines have a smaller average nuclear area in comparison to undamaged intestines. Data presented for a sample size of 24 - 28 intestines per treatment group, error bars show +/- SEM. Unpaired t-test, [t= 9.315, df= 51, p < 0.0001 (****)].
(B) Further analysis of the Slide Scanner images used in Fig. 14A, illustrated over a 24-hour period. Irradiated intestines consistently have a smaller nuclear area across all the time points when compared to the undamaged intestines. The data is presented for n = 6 - 8 intestines per treatment group and time point, error bars show +/- SEM. Two-way ANOVA [$F_{3,45}$= 1.973, p= 0.1316 (*n.s.)*]. Tukey's Multiple Comparison test comparing the undamaged to the damaged treatment groups: CT24 adjusted p value < 0.0001 (****); CT30 adjusted p value= 0.0041 (**); CT36 adjusted p value < 0.0001 (****); CT42 adjusted p value = 0.0445 (*).
(C) Quantification of the number of nuclei using Slide Scanner images of an area within the R5 intestinal region of *Drosophila* under free-running conditions. The irradiated intestines have a significantly larger number of nuclei present [unpaired t-test, t= 6.576, df= 51, p < 0.0001 (****)] in comparison to the undamaged intestines. The data is taken from a sample size of 24 - 28 intestines per treatment group and the error bars indicate +/- SEM.
(D) The same quantification was performed as in Fig. 14C, but presented as a 24-hour analysis. In accordance with Fig. 14C, the irradiated intestines consistently have a larger number of nuclei present across all time points in comparison to the undamaged group. Two of these time points yielded a significant difference: CT24 and CT36. Two-Way ANOVA, [$F_{3,45}$ = 1.675, p= 0.1858 (*n.s.)*]. Tukey's Multiple Comparison test comparing undamaged to irradiated groups: CT24 [adjusted p value = 0.0007 (***)]; CT30 [adjusted p value = 0.2974 (*n.s.*)]; CT36 [adjusted p value = 0.0026 (**)] and CT42 [adjusted p value = 0.5734 (*n.s.*)]. Data presented for a sample size of 6 – 8 intestines per treatment group, per time point, error bars represent +/- SEM.
(E) and (F) Bar graphs showing data obtained from quantifying an area in the intestinal R5 region of Slide Scanner images of *Drosophila* under free-running conditions. Quantifications were based on nuclear area, using 5µm^2 as the threshold cutoff to determine the percentage of total cells for each category. Undamaged intestines have an increased percentage of cells with a nuclear area greater than 5µm^2 in comparison to irradiated intestines [Fig. 14E, unpaired t-test t= 9.929, df= 51, p < 0.0001 (****)]. Irradiated intestines have significantly larger percentage of cells with a nuclear area less than or equal to 5µm^2 [Fig. 14F, unpaired t-test, t= 9.929, df= 51, p < 0.0001 (****)] in comparison to the undamaged intestines. Sample size of intestines quantified for Figures 14E and 14F are 24 - 28 intestines per treatment group, error bars represent +/- SEM.

3.1D Intestinal Permeability

The changes observed in intestinal nuclear morphology following exposure to irradiation prompted further investigation into the potential damage caused by irradiation at the tissue level.

A Smurf assay was used to assess if the cells become 'leaky' following irradiation. The control flies were raised under LD conditions and fed a 2.5% bromophenol blue solution for 24-hours prior to irradiation. *Drosophila melanogaster* have a pale yellow ventral abdomen, which is relatively transparent, allowing for *in vivo* visualization of the intestine after ingestion of the bromophenol blue solution. Under normal circumstances in an average aged fly, it is expected that the dye will be localized to the intestine. If the cells become damaged, it would be expected that the cellular integrity will be compromised causing increased intestinal permeability. In this case, the bromophenol blue dye would be expected to diffuse from the intestine and into the abdomen and no longer be localized from which the 'Smurf' assay name originates.

The level of 'smurfness' of each fly is determined by the amount of blue hue present in each fly. The categorization and naming of 'smurfness' was modified from a paper published by R. R. Martins and colleagues (Bio Protec) in 2018. Three categories were used to distinguish the flies, as shown in Figure 15. A fly characterized as a fully 'smurfed' fly would exhibit increased intestinal permeability resulting in diffusion of the bromophenol blue dye throughout the abdomen so that the dye is no longer localized to the intestine. In an intermediate 'smurfed' fly, the bromophenol blue dye has begun to diffuse from the intestine and is mainly present in the anterior portion of the abdomen. The last category is the low 'smurfed' fly in which the bromophenol blue dye is strictly localized to the intestine, such that the intestinal coil is clearly visualized. Figure 15 provides stereoscope images that are representative of each 'smurfness' category. Table #2 describes the 'smurfness' category observations at each time point post-irradiation for both the undamaged and damaged control flies. The low 'smurfed' categorization of smurfness was strictly seen in the undamaged samples across each time point analyzed. The majority of the intermediate 'smurfed' flies were observed in the *Drosophila* exposed to

irradiation. Two *Drosophila* that were exposed to irradiation began by showing characteristics of intermediately 'smurfed' flies, but were observed to exhibit 'fully' smurfed characteristics at three-hours post irradiation. Consequently, one of the fully 'smurfed' flies died as a result four-hours post irradiation.

FIGURE 15

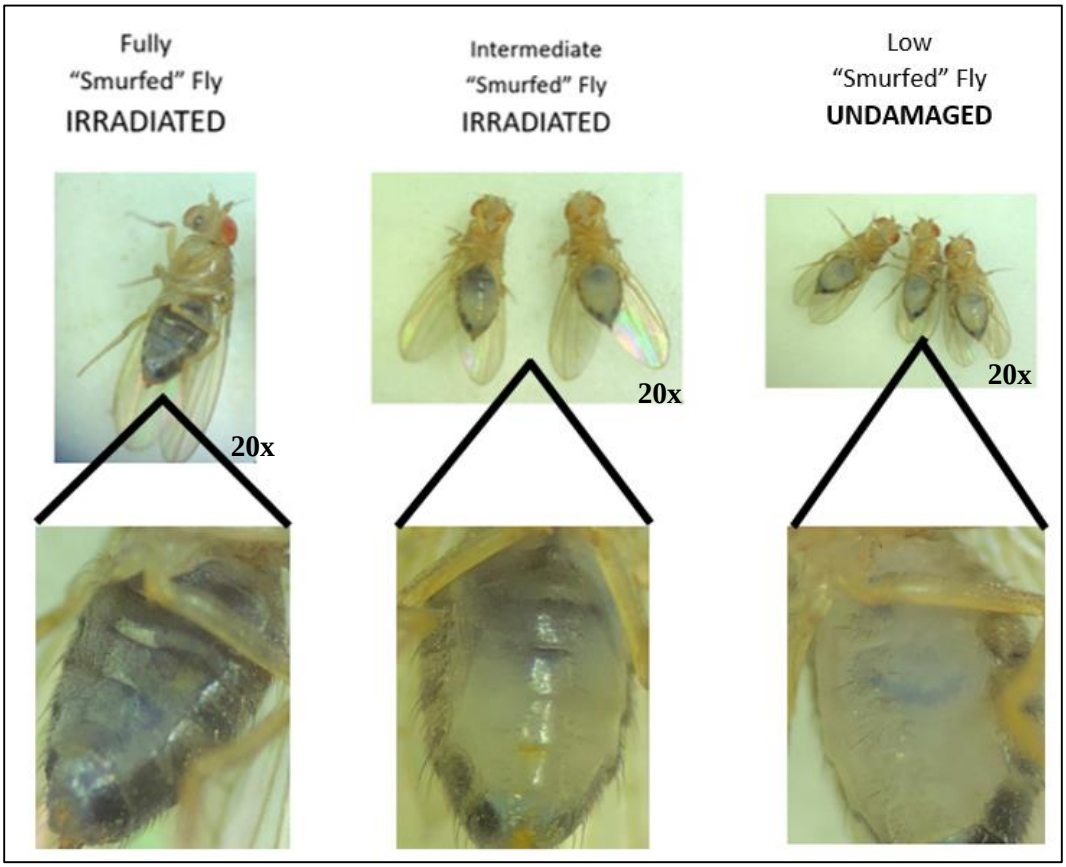

Figure 15: Characterization of *Drosophila* 'Smurfness' Levels
Representative images obtained from a stereoscope to illustrate each 'smurfness' category: fully 'smurfed', intermediate 'smurfed' and low 'smurfed' flies. Images were originally taken at 20x focus (top panel) but were electronically zoomed in (bottom panel) for clarity.

Table #2 Observations from Smurf Assay Flies were irradiated at ZT0 (7:00a.m.) and observed at various times throughout the day: immediately following irradiation (zero-hours post damage) to twenty-four-hours post irradiation. The table details the number of flies that fall under each 'smurfness' category at each time point observed.

Table #2 Observations from Smurf Assay

Time (Hour) Post-Irradiation	'Smurfness' Observations	
	UNDAMAGED	**IRRADIATED**
0	Low Level Smurfed: **18** Intermediately Smurfed: **0** Fully Smurfed: **0** Fully Smurfed Death: **0**	Low Level Smurfed: **18** Intermediately Smurfed: **0** Fully Smurfed: **0** Fully Smurfed Death: **0**
1	Low Level Smurfed: **18** Intermediately Smurfed: **0** Fully Smurfed: **0** Fully Smurfed Death: **0**	Low Level Smurfed: **18** Intermediately Smurfed: **0** Fully Smurfed: **0** Fully Smurfed Death: **0**
2	Low Level Smurfed: **18** Intermediately Smurfed: **0** Fully Smurfed: **0** Fully Smurfed Death: **0**	Low Level Smurfed: **0** Intermediately Smurfed: **18** Fully Smurfed: **0** Fully Smurfed Death: **0**
3	Low Level Smurfed: **18** Intermediately Smurfed: **0** Fully Smurfed: **0** Fully Smurfed Death: **0**	Low Level Smurfed: **0** Intermediately Smurfed: **16** Fully Smurfed: **2** Fully Smurfed Death: **0**
4	Low Level Smurfed: **18** Intermediately Smurfed: **0** Fully Smurfed: **0** Fully Smurfed Death: **0**	Low Level Smurfed: **0** Intermediately Smurfed: **15** Fully Smurfed: **2** Fully Smurfed Death: **1**
5	Low Level Smurfed: **18** Intermediately Smurfed: **0** Fully Smurfed: **0** Fully Smurfed Death: **0**	Low Level Smurfed: **0** Intermediately Smurfed: **15** Fully Smurfed: **2** Fully Smurfed Death: **1**
6	Low Level Smurfed: **18** Intermediately Smurfed: **0** Fully Smurfed: **0** Fully Smurfed Death: **0**	Low Level Smurfed: **0** Intermediately Smurfed: **15** Fully Smurfed: **2** Fully Smurfed Death: **1**
12	Low Level Smurfed: **18** Intermediately Smurfed: **0** Fully Smurfed: **0** Fully Smurfed Death: **0**	Low Level Smurfed: **0** Intermediately Smurfed: **15** Fully Smurfed: **2** Fully Smurfed Death: **1**
24	Low Level Smurfed: **18** Intermediately Smurfed: **0** Fully Smurfed: **0** Fully Smurfed Death: **0**	Low Level Smurfed: **0** Intermediately Smurfed: **15** Fully Smurfed: **2** Fully Smurfed Death: **1**
TOTAL NUMBER OF FLIES	**18**	**18**

Damaged flies were irradiated at ZT0 (7:00a.m.) and observed at various times throughout the day: immediately following irradiation (zero-hours post damage), one-hour post irradiation, two-hours post irradiation, three-hours post irradiation, four-hours post irradiation, five-hours post irradiation, six-hours post irradiation, twelve-hours post irradiation and twenty-four-hours post irradiation. Table #2 details the number of flies that fall under each 'smurfness' category at each time point observed, for a total sample of size of 18 flies per treatment group. Overall, the data showed that irradiation increased gut leakiness. Future research should explore irradiating the flies at different times of day and assessing their level of 'smurfness' accordingly. This would provide insight into the possible effects that time of damage may have on gut leakiness.

3.2 Is the JAK/STAT Stress Response Under Clock Control?

Next, I set out to determine if the JAK/STAT pathway is under 24-hour clock control. Both control flies (containing the STAT reporter) and period mutant flies (containing a STAT reporter) were raised in LD conditions and switched to DD conditions 24-hours prior to the experiment day. On the day of the experiment, the flies were irradiated at one of four different time points within a 24-hour period (CT24 = 7:00a.m., CT30 = 1:00p.m., CT36 = 7:00p.m. or CT42 = 1:00a.m.) to determine if the time that damage is incurred will have an effect on the JAK/STAT response. All flies were dissected three-hours post irradiation treatment. Slide scanner images were quantified and a GFP intensity threshold was set to be able to determine the ratio of GFP+ cells to DAPI+ cells. STAT reporter activity is identified within a cell is that is both GFP+ (indication of STAT activity) and DAPI+ (indicating the presence of a cellular nucleus). Two separate replicates, with five to seven flies per time point in each replicate, were

performed on this assay. A representative slide scanner image panel taken of the R5 region of *Drosophila* that were irradiated at CT42 is shown in Figure 16A. It is evident that there is a decreased number of GFP+ cells in the undamaged sample, in comparison to the damaged sample. The merge panel shows that despite many DAPI+ nuclei present in the undamaged sample, many of these nuclei are lacking STAT reporter activity. The merge panel also confirms that the GFP+ cells in the undamaged and irradiated panels are DAPI+.

Quantification of all the slide scanner images was performed to verify the qualitative observations described in Figure 16A. A graphical representation of the undamaged control and period mutant groups at each time point is illustrated in Figure 16B whereas Figure 16C is a graphical representation of the damaged control and period mutant groups at each time point. For the undamaged groups, the values for the ratio of GFP+ cells to total cells remains relatively constant for each treatment group across the time points, such that the ratio value for the control groups is around 0.05 and the ratio value for the period mutant groups is around 0.01 (Figure 16B). Additionally, the ratio of GFP+ cells to total cells in the undamaged control are significantly greater than the ratio of GFP+ cells to total cells in the undamaged period clock mutant [two-way ANOVA, p value < 0.0001 (****)]. In three of the time points (CT24 = 7:00a.m., CT36 = 7:00p.m. and CT42 = 1:00a.m.), the ratio of GFP+ cells to total cells is significantly larger in the control groups in comparison to the period mutant groups. At CT30, the GFP+ cells to total cells ratio is also elevated in the control group in comparison to the period mutant group, but this difference is not statistically significant. This suggests JAK/STAT activity is positively regulated by PER, and in its absence is at a low level, but that it is not time dependent.

The damaged treatment groups (graphed in Figure 16C), indicate that across each of the time points, the ratio values of GFP+ cells to total cells in the control groups are larger than the ratio values in the period mutant groups. Unlike Figure 16B, the ratio values for the control groups in Figure 16C fluctuate across each time point and differ depending on the time of irradiation, whereas the ratio values for the period mutant groups remain consistently similar across each time point (a ratio value of approximately 0.02). In Figure 16C, a statistically significant difference is noted in the irradiated control at CT30 versus the irradiated control at CT42 [two-way ANOVA, adjusted p value = 0.0080 (**)]. This suggests that there could be a time dependent difference in JAK/STAT activity levels following irradiation.

FIGURE 16

A

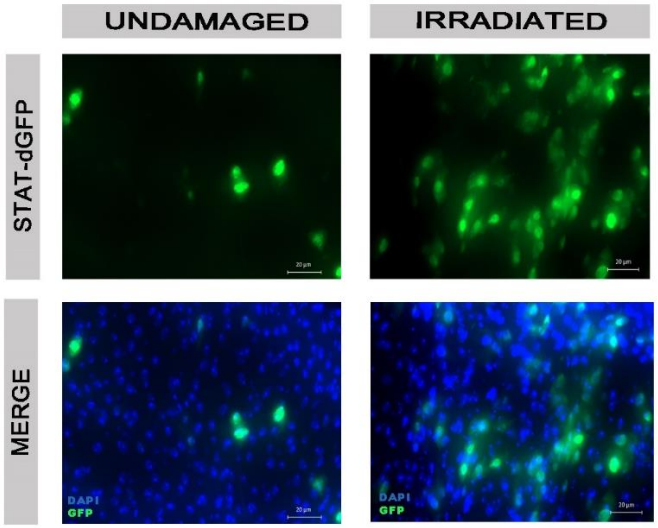

B

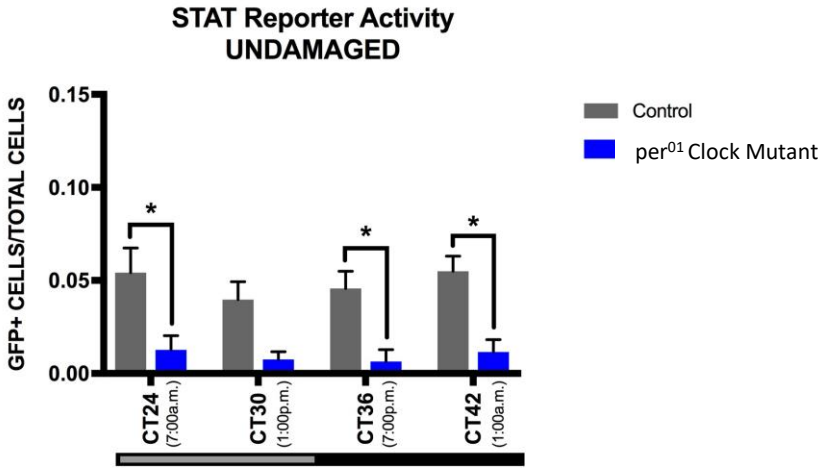

C

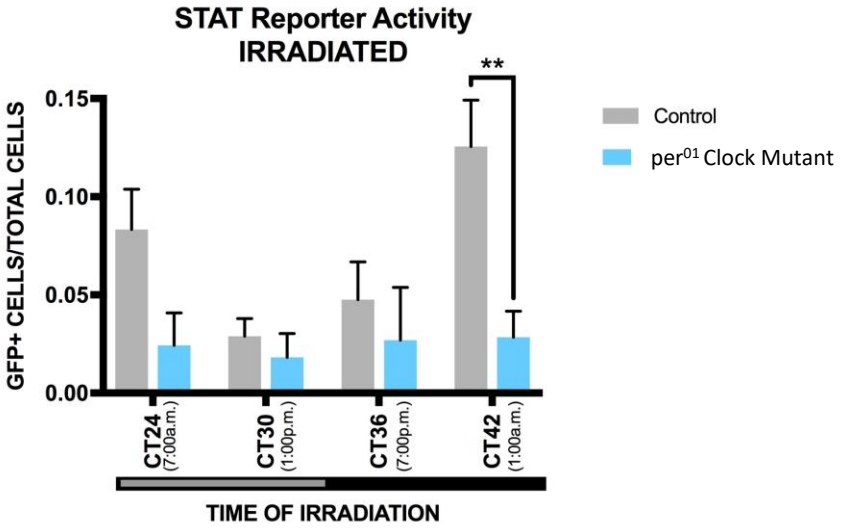

Figure 16: Following Irradiation, the Circadian Clock Regulates the JAK/STAT Pathway in a Time Dependent Manner
(A) Slide scanner image panel of representative images of the *Drosophila* R5 Region for the undamaged and irradiated treatment groups at CT42. Dissections were performed three-hours post-irradiation (CT45). GFP+ cells mark STAT reporter activity and DAPI is used as a nuclear counterstain. Scale bar represents 20μm.
(B) Analysis of the slide scanner images of the undamaged control and period mutant groups to determine the average ratio of GFP+ cells (marked in green) to the total number of cells (marked in blue, DAPI). Period regulates the JAK/STAT reporter in a non-time dependent manner. Data presented for n = 8 – 12 intestines per group, per time point from two separate replicate experiments. Error bars show + SEM. Two-way ANOVA [$F_{3,79} = 0.151$, $p = 0.9287$ *(n.s.)*]. Tukey's Multiple Comparison Test comparing the control group to period mutant group: CT24 adjusted p value = 0.0223 (*), CT30 adjusted p value = 0.2071 (*n.s.),* CT36 adjusted p value = 0.0485 (*) and CT42 adjusted p value = 0.0231 (*).
(C) Quantification of slide scanner images from the damaged control and period mutant groups to investigate the average ratio of GFP+ cells (marked in green) to the total number of cells (DAPI+, marked in blue). Following irradiation damage, the circadian clock will regulate the JAK/STAT pathway in a time-dependent manner. Data presented for n = 8 – 12 intestines per group, per time point from two separate replicate experiments. Error bars show + SEM. Two-way ANOVA [$F_{3,80} = 2.287$, $p = 0.0849$ *(n.s.)*]. Tukey's Multiple Comparison Test comparing the control group to the period mutant group: CT24 adjusted p value = 0.4324 (*n.s.),* CT30 adjusted p value > 0.9999 (*n.s.*), CT36 adjusted p value = 0.9925 (*n.s.*) and CT42 adjusted p value = 0.0074 (**).

3.3 Is Bacterial Presence Required for JAK/STAT Activity?

It has previously been shown that the JAK/STAT pathway is activated in response to bacterial infection (Buchon *et al.*, Cell Host Microbe, 2009). I sought to determine if the JAK/STAT response seen in Figure 16 is a result of the irradiation or a response to the bacterial presence in the midgut. It is unclear whether the intestinal stress response is a direct response from the damage caused by irradiation or an indirect effect due to the presence of bacteria in the intestine, which in turn, causes an inflammatory response. To further investigate the cause of the intestinal JAK/STAT response, an axenic assay was developed. The purpose of this assay was to eliminate as much bacteria as possible and then repeat the irradiation assay to be able to

determine the root of the response—either from irradiation or bacteria. To accomplish axenic conditions, eggs laid by control flies (containing the STAT-dGFP reporter) and period mutant flies (with the STAT-dGFP reporter) were collected from apple juice agar. The collected eggs underwent a bleaching step were placed in an autoclaved vial containing a cocktail of antibiotics that were supplemented into regular fly food. The eggs were raised until eclosion. Once the flies had emerged from their pupal casing, they were transferred to new vials. These flies were raised in LD conditions and 24-hours prior to experimentation, they were moved to DD conditions, in accordance with the standard irradiation protocol. On the day of the experiment, control and period mutant flies were irradiated at one of two time points within a 24-hour period: CT30 (1:00p.m.) or CT42 (1:00a.m.). Three-hours post irradiation, the flies were dissected and mounted. Once the slides were dry, they were scanned on a Slide Scanner for quantification.

Representative slide scanner images for both damaged and undamaged treatments are shown in Figure 17A for the control flies and Figure 17B for the period mutant flies. In Figure 17A, it is evident that there are no significant differences between the undamaged flies fed antibiotic food in comparison to the damaged flies fed antibiotic food. This is true for both time points (CT30 and CT42). Interestingly, there are very little to no GFP+ cells (which would be indicative of STAT reporter activity) present in the undamaged or damaged treatment groups. A similar trend is seen in the period mutant image panel in Figure 17B, where very little to no GFP+ cells are evident in the undamaged flies fed antibiotic food nor in the damaged flies fed antibiotic food at either time points.

Analysis of the slide scanner images was performed to determine the average ratio of GFP+ cells to total cells for each treatment group. Figure 17C is a graphical representation of the treatment groups at the CT30 time point and Figure 17D is a graphical representation of the

treatment groups at the CT42 time point. It is evident that at CT30 and CT42, the axenically treated flies have extremely little to no GFP+ cells present (Figures 17 C – D) yielding a ratio value of GFP+ cells to total cells to essentially be zero across all axenically handled groups regardless if they were irradiated or not. This supports the observations noted in the representative images featured in Figures 17 A – B. At the CT30 time point, significant differences are noted between the undamaged control and axenic undamaged control as well as between the irradiated control and axenically irradiated control. At the CT42 time point, the only significant difference is noted between the damaged control and the axenic damaged control.

FIGURE 17

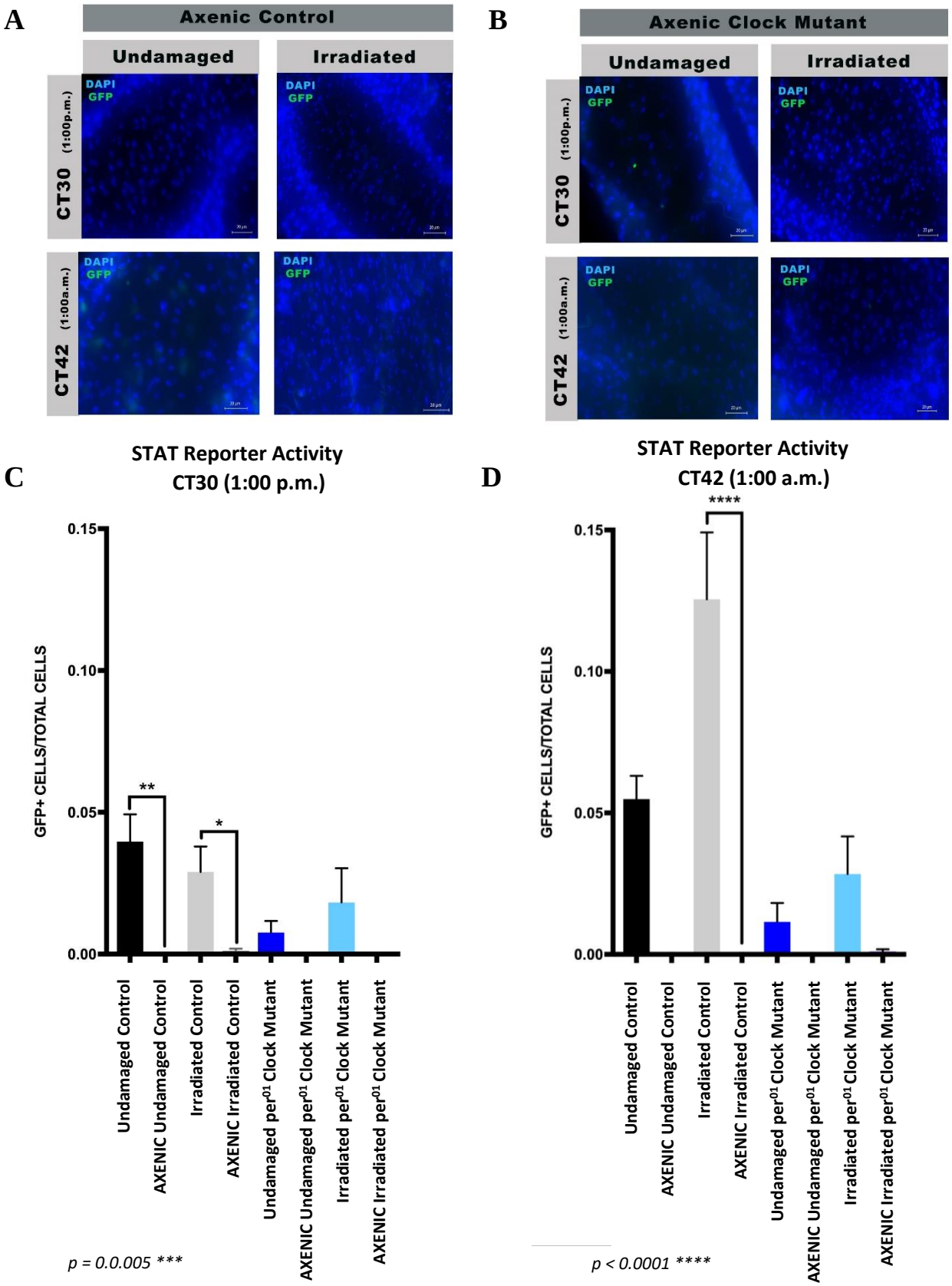
A
Axenic Control
Undamaged
Irradiated
CT30 (1:00p.m.)
CT42 (1:00a.m.)
DAPI
GFP
B
Axenic Clock Mutant
Undamaged
Irradiated
CT30 (1:00p.m.)
CT42 (1:00a.m.)
DAPI
GFP
C
STAT Reporter Activity
CT30 (1:00 p.m.)
GFP+ CELLS/TOTAL CELLS
0.15
0.10
0.05
0.00
**
*
Undamaged Control
AXENIC Undamaged Control
Irradiated Control
AXENIC Irradiated Control
Undamaged per01 Clock Mutant
AXENIC Undamaged per01 Clock Mutant
Irradiated per01 Clock Mutant
AXENIC Irradiated per01 Clock Mutant
p = 0.0.005 ***
D
STAT Reporter Activity
CT42 (1:00 a.m.)
GFP+ CELLS/TOTAL CELLS
0.15
0.10
0.05
0.00
****
Undamaged Control
AXENIC Undamaged Control
Irradiated Control
AXENIC Irradiated Control
Undamaged per01 Clock Mutant
AXENIC Undamaged per01 Clock Mutant
Irradiated per01 Clock Mutant
AXENIC Irradiated per01 Clock Mutant
p < 0.0001 ****

Figure 17: Bacteria Are Required for JAK/STAT Activity.
(A - B) Representative slide scanner images for control flies (A) or period mutant flies (B) raised on antibiotic (AB) supplemented food. Image panel showcases both undamaged and damaged treatment groups at both time points (CT30 and CT42), where DAPI+ cells (nuclear counterstain) are marked in blue and GFP+ cells (STAT reporter) are in green. Very little to no GFP+ cells are present in the flies raised with the antibiotic-supplemented food. Scale bar represents 20µm.
(C - D) Graphical analyses of slide scanner images described above. Axenically raised flies have no JAK/STAT activity regardless if the flies are damaged or undamaged. This suggests that bacteria are required to elicit a JAK/STAT response. Data presented for n = 8 – 12 intestines per treatment group (Fig. 17C) and n = 6 – 10 intestines per treatment group (Fig. 17D), error bars show + SEM.
Fig. 17C: One-Way ANOVA [$F_{7,68} = 4.365$, $p = 0.0005$ (***)]. Brown-Forsythe Test: undamaged control vs. axenic undamaged control p value = 0.0039 (**), irradiated control vs. axenic irradiated control p value = 0.0417 (*).
Fig. 17D: One-Way ANOVA [$F_{7, 69} = 13.93$, $p < 0.0001$ (****)]. Brown- Forsythe Test: irradiated control vs axenic irradiated control p value < 0.0001 (****).

To test the efficacy of the antibiotic-supplemented fly food, a sterile polyester tipped applicator (Fisher Scientific, cat. no. 25-806) was used to obtain a sample from the surfaces of antibiotic-supplemented fly food and regular fly food. The applicator was then streaked onto a Tryptic Soy Agar (TSA) plate. The inoculated plates were placed in a 37°C bacterial incubator (Quincy Lab Inc., Model #10-140) and observed for growth 24- and 48-hours post-inoculation.

Images of the corresponding petri dishes are shown below in Table #3. There is increased bacterial growth visible on the TSA plate streaked with the regular fly food sample at both 24 and 48 hours post-streaking, with 36 colonies visible at 24-hours post streaking and 31 colonies visible at 48-hours post streaking. The colonies observed at 48-hours post streaking appear to be larger in size (when compared to 24-hours post streaking) and some may have combined with neighbouring colonies. No bacterial growth was present on the TSA plates streaked with the antibiotic-supplemented fly food sample at 24 and 48 hours post streaking.

Table #3 Bacterial Growth Observations of Samples Obtained from Fly Food Growth of bacteria from vials housing *Drosophila* (that eclosed from bleached eggs) raised on antibiotic-supplemented fly food or housing *Drosophila* (that eclosed from bleached eggs) raised on regular fly food was observed on TSA plates after 24-hours post streaking and 48-hours post streaking.

	Antibiotic-Supplemented Food Sample	**Regular Food Sample**
24 Hours Post	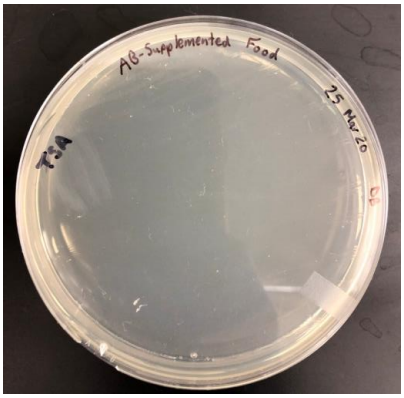 Number of Colonies = 0	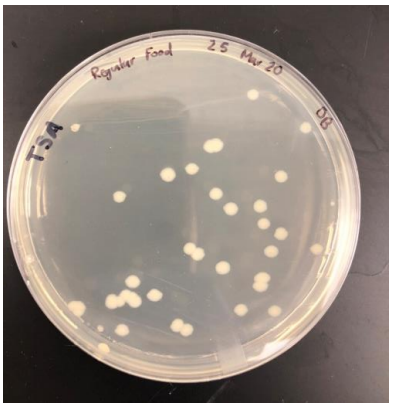 Number of Colonies = 36
48 Hours Post	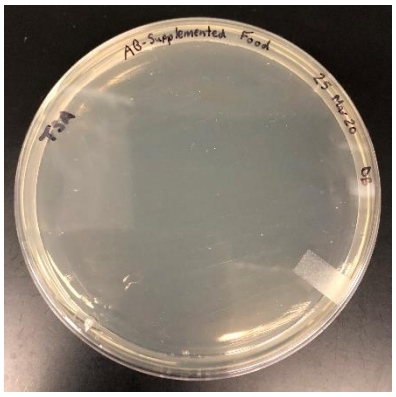 Number of Colonies = 0	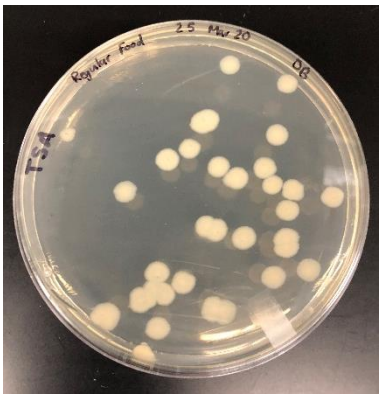 Number of Colonies = 31

3.4 Does Superoxide Presence Vary Throughout the Day Following Irradiation Damage?

Superoxides are produced naturally as byproducts of mitochondrial metabolism (Miwa *et al.*, Free Radic Biol Med, 2003), but accumulation of high levels of superoxides can be harmful to an organism. Yamaguchi and Kashiwakura previously showed that x-ray irradiation causes a significant increase in the levels of intracellular ROS in cell culture studies (PLoS One, 2013). I therefore tested if irradiation produces a time dependent response. The presence of superoxides in the *Drosophila* intestine was detected using DHE staining dye.

To first ensure the DHE dye was detectable in the *Drosophila* intestine, control (; $\frac{6XSTAT-dGFP}{+}$;) and period mutant (per^{01}; $\frac{6XSTAT-dGFP}{Cyo}$;) female flies were exposed to different levels of hydrogen peroxide (0.5mg/mL and 2mg/mL) on Whatman glass microfiber filter paper, 24mm (Millipore Sigma, cat. no. WHA1821024) 24-hours prior to the experiment day. A representative image panel showcasing the positive and negative controls used are shown in Figure 18 to verify the effectiveness of using this particular dye. The undamaged sample was used as a negative control, which showed little DHE+ cells. A 2% of hydrogen peroxide (H_2O_2) solution was used as the positive control treatment. It was evident that the 2% H_2O_2 solution had an increased population of DHE+ cells in the posterior intestinal R4/ R5 region and the anterior intestinal R1 region, so this was used as the standard for increased DHE signal (as indicated by the white arrows in Figure 18). The levels of DHE+ cells in the irradiated groups was included in the Figure 18 image panel for comparison. The irradiated control and irradiated period mutant samples have less DHE+ cells present when compared to the positive control (Figure 18).

FIGURE 18

CT24 Undamaged (7:00a.m.) ------- Negative Control	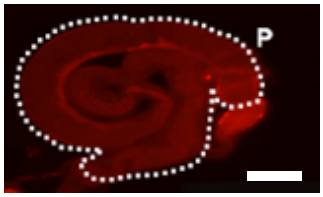
ZT3 2% H_2O_2 (10:00a.m.) ------- Positive Control	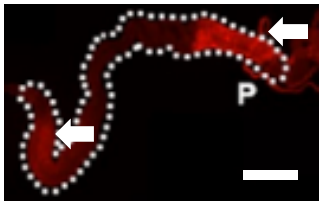
CT24 per^{01} Clock Mutant Irradiated (7:00a.m.)	
CT24 Control Irradiated (7:00a.m.)	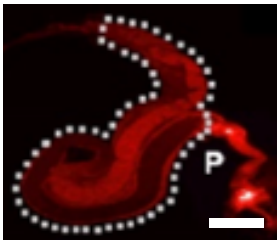

Figure 18: DHE Dye Verification
Various positive and negative controls were tested to verify the efficacy of DHE dye, which marks cells in red. Slide scanner representative images are shown above, where the entire intestine is outlined in white and the posterior portion of the intestine is marked with the letter 'P'. The undamaged sample was used as a negative control, which shows little DHE+ cells. The 2% H_2O_2 solution was used as a positive control, showing increased DHE+ cells, especially in the posterior region. Areas of increased DHE+ cells are indicated by the white arrows. Scale bar represents 200µm.

To determine the optimal time to observe the DHE staining after damage, the flies were dissected at various time points post irradiation (one-hour post irradiation, two-hours post irradiation, three-hours post irradiation, four-hours post irradiation, five-hours post-irradiation and six-hours post irradiation) and subsequently viewed under a fluorescent microscope to observe the slides for DHE+ cells. Ultimately, it was determined that a dissection of three hours post irradiation would be most optimal due to the limited half-life of DHE dye and the DHE intensity levels observed were brightest at that time.

Following verification of the DHE staining protocol, the irradiation assay was performed to investigate any time of day dependence on superoxide presence. Control and period mutant flies were raised in LD conditions and moved to DD conditions 24-hours prior to the experiment date. On the day of the experiment, the flies were irradiated at one of four different time points (CT24 = 7:00a.m., CT30 = 1:00p.m., CT36 = 7:00p.m. or CT42 = 1:00a.m.) and then dissected three-hours post irradiation. DHE and DAPI staining was performed. The slides were scanned on a slide scanner the next day so that the images could be appropriately quantified before the signal degradation occurred. This assay was replicated two separate times.

Analysis of the slide scanner images yielded the graphical representations seen in Figures 19 C – D. An average ratio value of the total number of DHE+ cells (marked in red) to the total number of cells (marked by DAPI in blue) was determined for the intestinal R5 region of each intestinal sample analyzed. There are no statistically significant differences between the ratio of DHE+ cells to the total number of cells in either undamaged or irradiated conditions. Interestingly, it appears that the undamaged group has a larger number of DHE+ cells present when the ratio levels of DHE+ cells in the undamaged group to the irradiated group are compared, although these differences are not significant. By comparing the treatments

performed for each condition, it appears that under undamaged conditions, the control group (Figure 19 C) has a larger number of DHE+ cells in comparison to the clock mutant group. The value of DHE+ cells to total cells also appears to fluctuate throughout the day in the undamaged control group, despite the differences not being statistically significant. Additionally, the undamaged clock mutant appears to be arrhythmic and show no patterns of time of day dependence.

FIGURE 19

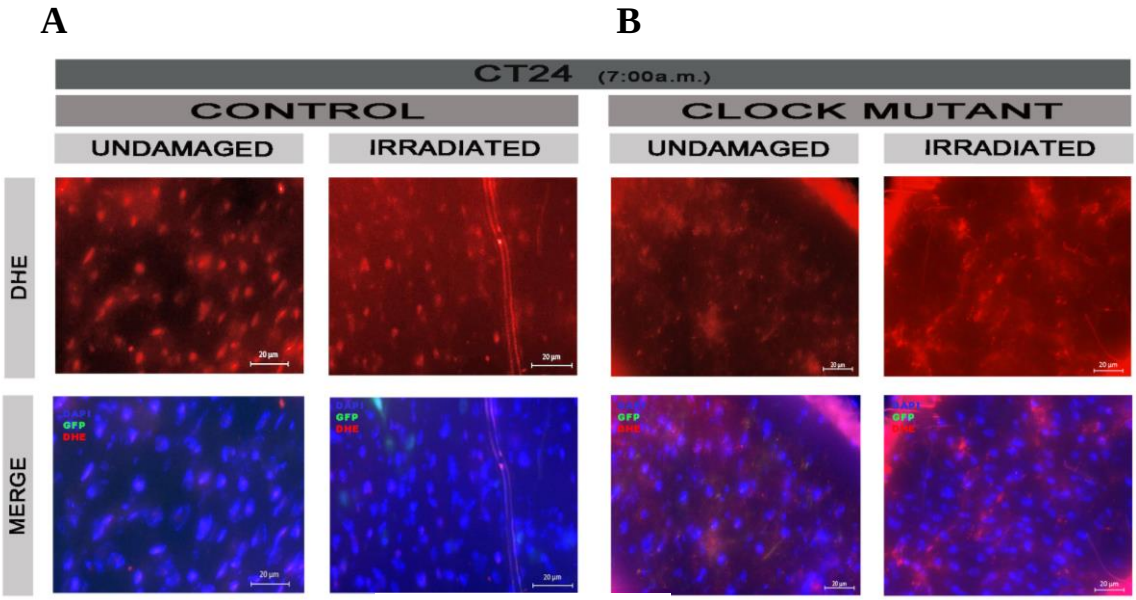
A
B
CT24 (7:00a.m.)
CONTROL
CLOCK MUTANT
UNDAMAGED
IRRADIATED
UNDAMAGED
IRRADIATED
DHE
MERGE

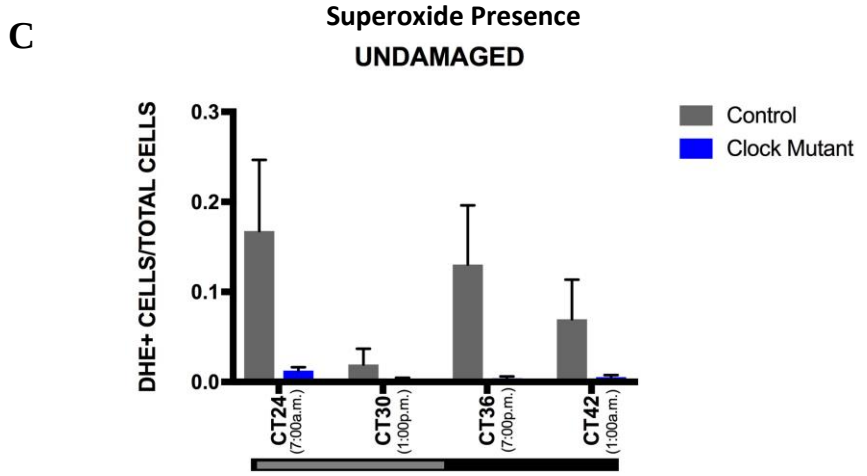
C
Superoxide Presence
UNDAMAGED
DHE+ CELLS/TOTAL CELLS
0.3
0.2
0.1
0.0
CT24 (7:00a.m.)
CT30 (1:00p.m.)
CT36 (7:00p.m.)
CT42 (1:00a.m.)
Control
Clock Mutant

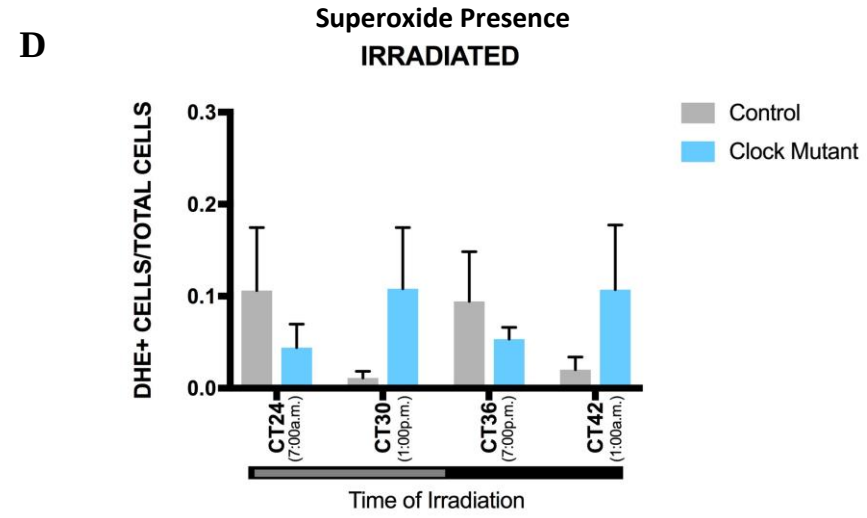
D
Superoxide Presence
IRRADIATED
DHE+ CELLS/TOTAL CELLS
0.3
0.2
0.1
0.0
CT24 (7:00a.m.)
CT30 (1:00p.m.)
CT36 (7:00p.m.)
CT42 (1:00a.m.)
Time of Irradiation
Control
Clock Mutant

Figure 19: Irradiation Does Not Affect Superoxide Generation and Superoxide Presence Does Not Significantly Vary Throughout the Day
(A) Representative slide scanner images of intestinal R5 region in control flies at CT24 (7:00a.m.) under damaged and undamaged conditions. DHE+ cells are in red (indicating superoxide presence), GFP+ cells are in green (indicating STAT activity) and DAPI+ cells are in blue (nuclear counterstain). The number of DHE+ cells appears to be slightly less in the damaged treatment group when compared to the undamaged treatment group. Scale bar is set to 20µm.
(B) Slide scanner image panel of representative pictures of the intestinal R5 region in period mutant flies at CT24 under undamaged and damaged conditions. Scale bar is set to 20µm.
(C) Analysis of slide scanner images for undamaged treatment groups across each time point. In the control groups, superoxide presence does not significantly vary depending on time of day. Data presented for 7 – 12 intestines per group per time point, error bars represent + SEM. Two-way ANOVA [$F_{3,58} = 1.126$, $p = 0.3460$ (*n.s.)*].
(D) Analysis of slide scanner images for damaged treatment groups across each time point. Irradiation does not increase superoxide production. Data presented for 7 – 12 intestines per group, per time point, error bars represent + SEM. Two-way ANOVA [$F_{3,65} = 1.602$, $p = 0.1974$ (*n.s.)*].

3.5 Is There Clock Dependence on the JAK/STAT Pathway?

Manipulations to different components of the JAK/STAT pathway have previously been shown to change circadian behavioural rhythms (Luo *et. al*, Cell, 2012). To gain a better understanding of the relationship between the circadian clock and the JAK/STAT pathway, I tested if activation of the JAK/STAT pathway (by unpaired overexpression) has any effect on clock function. A *Drosophila* strain that overexpressed unpaired cytokine (UPD) with a clock reporter background was constructed using the UAS-GAL4 *Drosophila* system. The UAS/GAL4 gene expression system functions through an effector transgene that is linked to a promoter containing an upstream activator sequence (UAS), allowing control over the regional and temporal expression of the transgene (Figure 20). $GAL80^{ts}$ is a temperature sensitive inhibitor, and at restrictive conditions (temperatures less than 19°C), the activity of GAL4 is inhibited, causing suppression of the transgene (UPD). At permissive conditions, $GAL80^{ts}$

becomes nonfunctional and allows for the transcriptional activity of GAL4 to move forward (Fujimoto *et al.,* Developmental Dynamics, 2011). The transcriptional driver of GAL4 is myo1A, which is specific to expressing intestinal enterocytes, thus binding of GAL4 to UAS activates UPD overexpression in the intestinal enterocytes allowing for cell specificity.

FIGURE 20

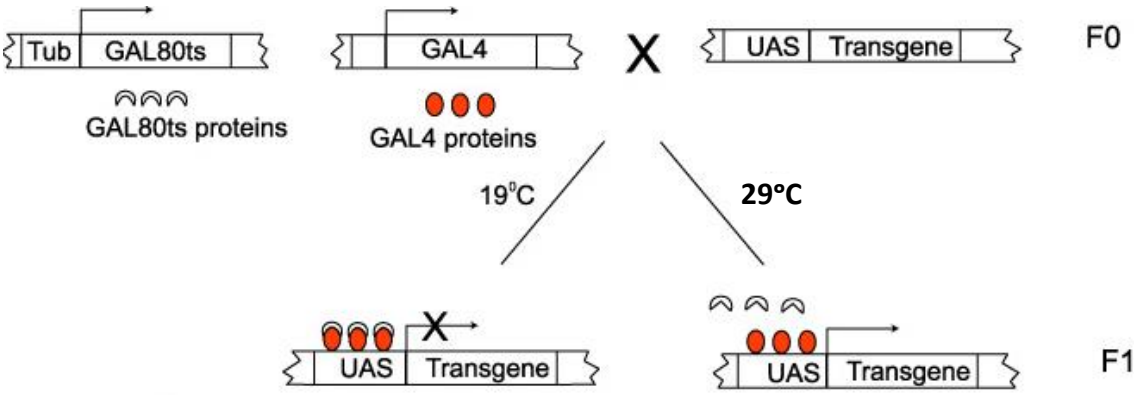

Modified from Wang & Zhong, [Perspective] Science, 2004

Figure 20: Schematic of the UAS/GAL4 System
Illustration depicts the UAS/GAL4 system under both restrictive conditions (at 19°C), where the transgene is not transcribed, and under permissive conditions (at 29°C), where the transcription of the transgene is permitted.

Upon eclosion, the desired flies were collected and shifted to a 29°C LD incubator for five days. At 29°C, the UAS-GAL4 system was activated to allow for the overexpression of UPD. After five days, the flies were dissected at eight different time points within a 24-hour period (ZT0 = 7:00a.m., ZT3 = 10:00a.m., ZT6 = 1:00p.m., ZT9 = 4:00p.m., ZT12 = 7:00p.m., ZT15 = 10:00p.m., ZT18 = 1:00a.m. and ZT21 = 4:00a.m.). The slides were scanned using a slide scanner and analyzed for quantification. Representative images are shown in Figure 21A.

Across all the time points analyzed, the intestines that overexpressed UPD were a lot smaller in length, but thicker in width and appeared to look distended, especially when compared to their control counterparts. This observation is consistent with the literature, in which unpaired overexpression causes an increase in intestinal stem cell proliferation, which is described to have a similar phenotype (Beebe *et al.*, Dev Biol, 2010). Figure 21A shows increased $Clock^{PER}$ reporter fluorescence (GFP+ cells) throughout all regions of the intestine in the UPD overexpression sample at ZT0.

Four regions were analyzed on each intestine sample: (a) entire intestine (b) posterior R5 region (c) anterior R1 region and (d) midgut R2 to R4 region. It is evident across the various analyses (Figures 21 B– E), that the average curve seen for the unpaired overexpression group has a stronger GFP to DAPI intensity ratio in comparison to the control. This suggests that the overexpression of unpaired increased the clock reporter signal.

Additionally, the average intensity ratio for UPD overexpression tends to follow a 'U'-shaped curve, where ZT0 (7:00a.m.) is a peak and a trough occurs between ZT12 (7:00p.m.) to ZT15 (10:00p.m.). The curve begins to peak again at ZT21 (4:00a.m.). The average ratio curve for the control groups across Figures 21 B – E is similar to the unpaired overexpression curve except it is a lot more dampened and the peaks and troughs are more difficult to distinguish. Across each figure, there appears to be a consistent peak at ZT3 (10:00a.m.) in the control group. The $Clock^{PER}$ rhythm for UPD overexpression is consistent with the $Clock^{PER}$ rhythm published by Parasram and colleagues (Stem Cell Rep, 2018).

FIGURE 21

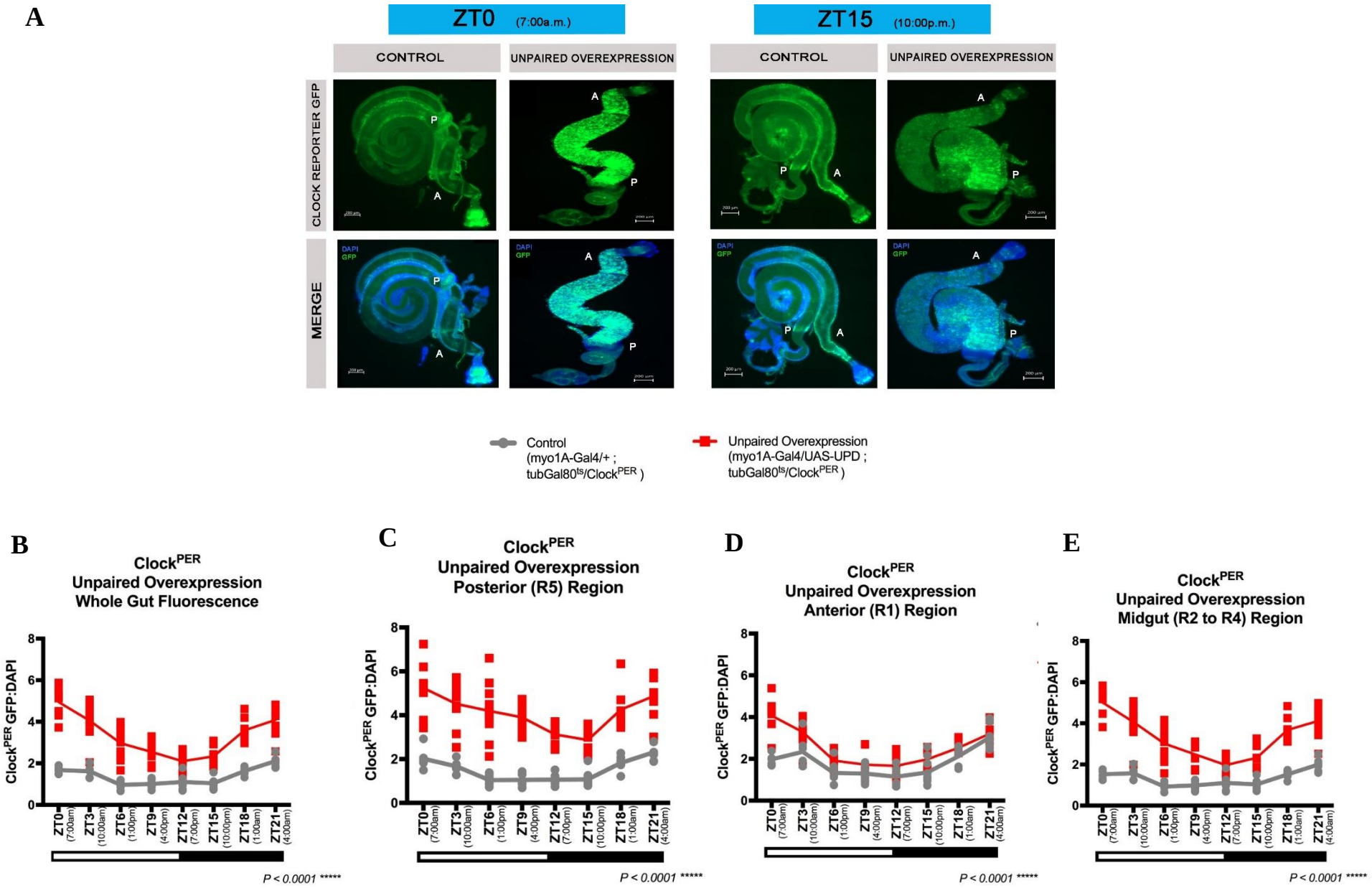
A
ZT0 (7:00a.m.)
ZT15 (10:00p.m.)
CONTROL
UNPAIRED OVEREXPRESSION
CONTROL
UNPAIRED OVEREXPRESSION
CLOCK REPORTER GFP
MERGE
DAPI
GFP
A
P
Control
(myo1A-Gal4/+ ;
tubGal80ts/ClockPER)
Unpaired Overexpression
(myo1A-Gal4/UAS-UPD ;
tubGal80ts/ClockPER)
B
ClockPER
Unpaired Overexpression
Whole Gut Fluorescence
ClockPER GFP:DAPI
P < 0.0001 *****
C
ClockPER
Unpaired Overexpression
Posterior (R5) Region
ClockPER GFP:DAPI
P < 0.0001 *****
D
ClockPER
Unpaired Overexpression
Anterior (R1) Region
ClockPER GFP:DAPI
P < 0.0001 *****
E
ClockPER
Unpaired Overexpression
Midgut (R2 to R4) Region
ClockPER GFP:DAPI
P < 0.0001 *****
ZT0 (7:00am)
ZT3 (10:00am)
ZT6 (1:00pm)
ZT9 (4:00pm)
ZT12 (7:00pm)
ZT15 (10:00pm)
ZT18 (1:00am)
ZT21 (4:00am)

Figure 21: The JAK/STAT Pathway Does Not Regulate the Circadian Clock
(A) Representative slide scanner image of whole gut fluorescence of $Clock^{PER}$ reporter at ZT0 (7:00a.m.) and ZT15 (10:00p.m.). Increased levels of GFP+ cells are visible throughout the unpaired overexpression sample at ZT0. Increased GFP+ cells are mainly in the posterior portion of the unpaired overexpression sample at ZT15. The Clock is still functional when unpaired is overexpressed. 'A' indicates the anterior portion of the intestine and 'P' indicates the posterior portion of the intestine, scale bar represents 200µm.
(B – E) Slide scanner image quantifications of GFP to DAPI Clock reporter intensities for the whole intestine (Fig. 21B), posterior region (Fig. 21C), anterior region (Fig. 21D) and midgut region (Fig. 21E) for flies overexpressing unpaired (red) and control flies (grey). The clock is still functional despite unpaired being overexpressed, implying that the JAK/STAT pathway does not regulate the circadian clock. Data presented for n = 6 – 10 intestines per treatment group, per time point. Two-Way ANOVA: Fig. 21A: [$F_{7,115} = 7.193$, $p < 0.0001$ (****)], Fig. 21B: [$F_{7,114} = 7.014$, $p = 0.0592$ (****)], Fig. 21C [$F_{7,113} = 4.166$, $p = 0.0004$ (****) and Fig. 21D: [$F_{7,111} = 8.111$, $p < 0.0001$ (****)].

3.6 Testing the JNK and Hippo Pathways

To further understand the circadian clock regulation of stress signaling, a JNK and Hippo reporters were obtained from the laboratory of Norbert Perrimon (Dept. of Genetics, Harvard Medical School). The JNK reporter strain worked in the *Drosophila* intestine, so it was tested following irradiation. The Hippo reporter did not work in the *Drosophila* intestine so no further experimentation took place using this reporter.

Drosophila were dissected at different times throughout their lifespan to determine a baseline level of endogenous JNK activity. An inverted fluorescent microscope was used to make qualitative observations and determine that the levels of JNK detected by the JNK reporter were very low throughout their lifespan (Figure 22). It was noted that some JNK activity was observed in the anterior midgut of older (29 and 35 day) flies, which is consistent with previous reports (Biteau *et al.,* Cell Stem Cell, 2011). JNK reporter flies were raised in LD conditions and on the day of the experiment, all the fly groups were irradiated at ZT0 (7:00a.m.). Dissections occurred at different times post irradiation damage: ZT1 (8:00a.m.), ZT2 (9:00a.m.), ZT3

(10:00a.m.), ZT4 (11:00a.m.), ZT5 (12:00p.m.), ZT6 (1:00p.m.), ZT9 (4:00p.m.), ZT12 (7:00p.m.), ZT18 (10:00p.m.) and ZT24 (7:00a.m. the following day). No clearly marked GFP+ cells were present at any of the dissection times for the JNK reporter. At ZT4, there appeared to be some cells with faint GFP+ cells but the GFP did not stain as previous GFP stains have been traditionally known to stain. The GFP stain appeared to only mark the outer circumference of most cells giving the appearance that the cells were faintly outlined. Overall, the observations yielded no difference in JNK reporter activity across the time points following irradiation. A representative slide scanner image of the visualizations of the JNK reporter at each time point dissected after being subjected to irradiation is shown in Figure 22B.

FIGURE 22

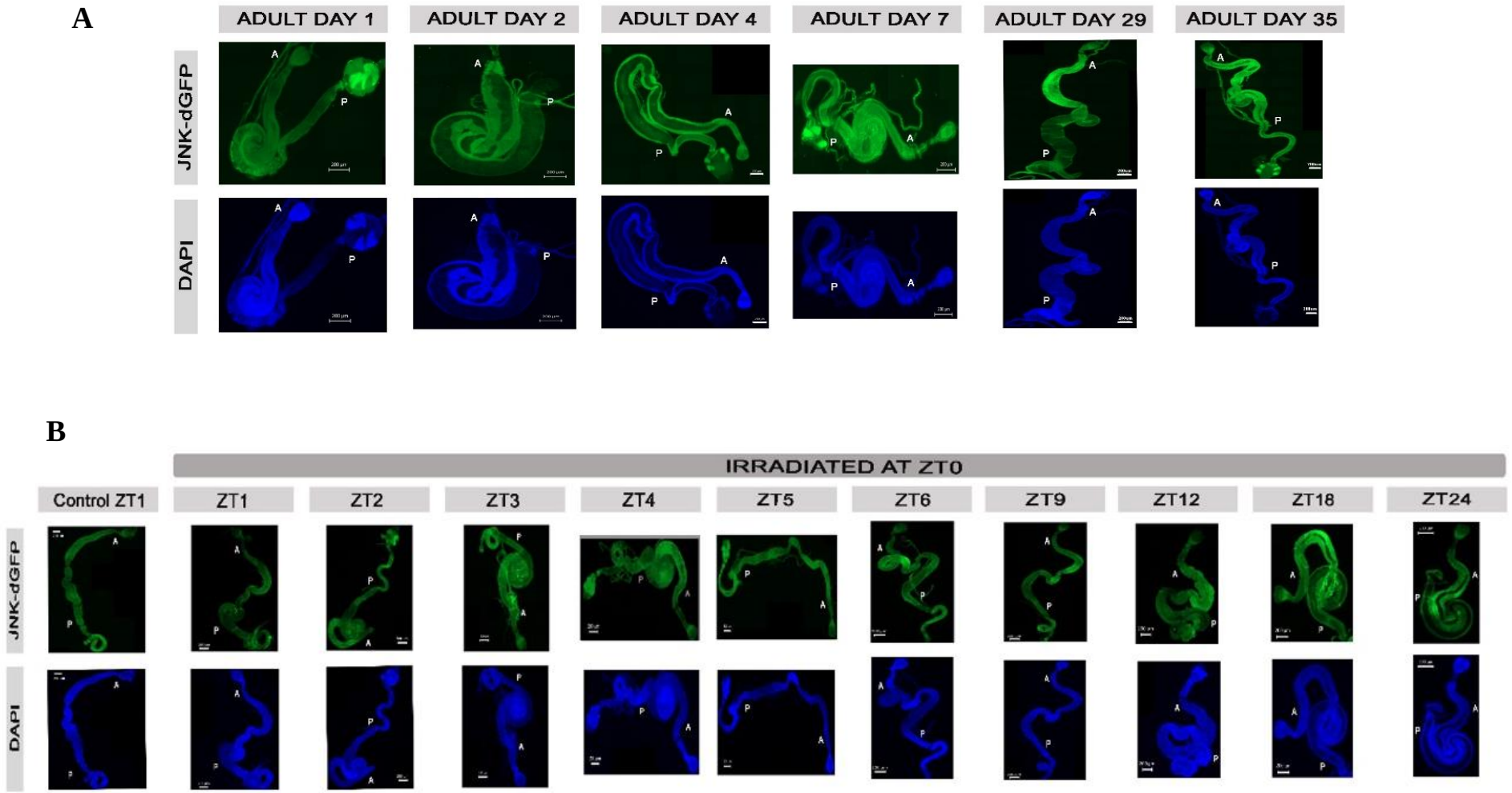

Figure 22: JNK Activity May Be Present in the Older Stages of *Drosophila* Development and There Are No Time Dependent Changes in JNK Activity Following Irradiation

(A) Representative slide scanner images from undamaged treatment of whole gut fluorescence in the JNK-dGFP reporter. The anterior portion of the older flies (Adult Day 29 and Adult Day 35) appear to have some GFP fluorescence anteriorly, but the signal is low and cannot be positively identified as positive reporter activity. 'A' indicates the anterior portion of the intestine and 'P' indicates the posterior portion of the intestine, scale bar represents 200µm.
(B) The representative slide scanner images of whole gut fluorescence of the JNK reporter flies irradiated at ZT0 and dissected at the corresponding times following irradiation. JNK reporter activity is not present in intestines following exposure to irradiation. Presence of the JNK reporter activity would have be marked in green (GFP+ cells). 'A' indicates the anterior portion of the intestine and 'P' indicates the posterior portion of the intestine, scale bar represents 200µm.

CHAPTER 4

DISCUSSION

The JAK/STAT pathway is part of the *Drosophila* immune response (Agaisse & Perrimon, Immunol Rev, 2004). For example, cellular damage or injury can allow bacteria to enter the *Drosophila* hemolymph (blood system), causing an inflammatory response (Agaisse & Perrimon, Immunol Rev, 2004). Detection of the bacteria causes phagocytic white blood cells, called hemocytes, to release UPD cytokines that activate the JAK/STAT signalling pathway to promote cellular proliferation and regeneration of the lost cells (Agaisse & Perrimon, Immunol Rev, 2004). The JAK/STAT pathway plays an important role in the intestine due to its involvement in cellular proliferation and stem cell differentiation (Beebe *et al.,* Dev Biol, 2010). Previous studies have demonstrated the regenerative ability of the *Drosophila* intestine following chemical damage (ingestion of Bleomycin) and bacterial infection of *Erwinia carotovora carotovora 15 (Ecc15)* (Panayidou & Apidianakis, Pathogens, 2013) which reveals that inflammation is necessary for regeneration.

There is an important and poorly understood timing to inflammation and regeneration. Variations in *Drosophila* survival outcome have been associated with time of bacterial infection. Stone and colleagues (PLoS Path, 2012) injected *Drosophila* with *Staphylococcus aureus* either during the day or at night. They discovered that the flies injected at night had greater phagocytic activity than the flies injected during the day. Phagocytic activity is a protective cellular mechanism to destroy pathogens and a part of the *Drosophila* immune response. This indicates that the immune response varies depending on time of day. One research report has suggested that there may be a relationship between the circadian clock and the JAK/STAT pathway. Luo and colleagues (Cell, 2012) showed that manipulations to JAK/STAT pathway components, such

as downregulating UPD, could alter circadian behavioural rhythms. The involvement of the JAK/STAT pathway in the immune response encouraged me to explore if the JAK/STAT pathway is also under circadian clock control. This project set out to explore the possible time dependent changes in JAK/STAT activity by exploring the relationship between the JAK/STAT pathway and the circadian clock.

4.1 Implications of Irradiation on the Drosophila Intestinal Epithelium

An acute irradiation damage assay was developed to initiate the JAK/STAT pathway response. This damage assay was advantageous because it permitted the tracking of reporter activity throughout the day. Four different properties (survival, JAK/STAT reporter activity levels, nuclear damage and intestinal permeability) were tested to determine the effects of irradiation exposure and investigate the extent of damage both physiologically and at a cellular level.

Various factors can affect longevity of flies, including sex (males typically live shorter than females), temperature (lifespan shortens as temperature is increased) and vial cleanliness (dirty vials due to irregular vial flipping will shorten their lifespan) (Linford *et al.*, J Vis Exp, 2013). X-ray irradiation has been shown to negatively affect survival in animals, for example, mice administered 16Gy of irradiation have a mortality rate of 100% by day six post damage induction (Booth *et al.*, Health Phys, 2012). In comparison, *Drosophila* survival has been shown to be more resistant to irradiation damage and larvae have been shown to have robust survival following irradiation (Verghese & Su, PLoS Biol, 2016). Typically, under undamaged conditions female *Drosophila melanogaster* have a life span greater than 60 days if raised in a 25^{o}C incubator (Linford *et al*., J Vis Exp, 2013). A variation in survival was observed depending

on the time of irradiation. Control flies irradiated at ZT0 (7:00a.m.) showed a decrease in survival at day 50 that was not observed in the other treatments. The time of day variations observed may be an indication that there is a circadian clock influence on survival after irradiation. In addition, the clock mutant undamaged and irradiated flies had a decreased lifespan when compared to the control. This is consistent with previously published data by Klarsfeld & Rouyer (J Biol Rhythm, 1998) as well as Krishnan and colleagues (Aging Albany NY, 2009) which suggest that PER may play a role in extended longevity and healthspan. These findings contradict recently published data by Ulgherait and colleagues (Nat Commun, 2020), who showed that mutations in PER increase longevity due to their dependence on mitochondrial uncoupling for cellular respiration. My results further support an early circadian study performed by Halberg and colleagues in 1960 (Exp Biol Med). Halberg inoculated mice with an endotoxin at various times of day and recorded their survival. Mice inoculated at 12:00am.m had a survival rate greater than 90% whereas the survival of the mice inoculated at 4:00p.m. was less than 20% due to septic shock. Overall, my data confirm that PER loss decreases longevity and time of day variation in irradiation damage influence survival.

In addition to its roles in cellular proliferation, the JAK/STAT pathway also has roles in cellular differentiation, where it has more of a 'housekeeping' role to replace old cells. This means that baseline levels of JAK/STAT activity are expected to be present in a cell. Following damage, it is expected that JAK/STAT activity levels would increase as it switches over to a proliferation role to quickly replace the damaged cells. Irradiation damage resulted in increased JAK/STAT activity levels at three-hours and four-hours post irradiation. Although the increases were not significant, three-hours post irradiation was chosen as the time to study JAK/STAT activity because it would not overlap with other time points. For the time series experiment

conducted, time points occurred every six hours, so when factoring in the time to wait post irradiation prior to dissecting and the time it takes to perform the dissection, three-hours post irradiation would be most appropriate.

Exposure to irradiation is damaging to cells and may result in negative cellular consequences, such as apoptosis (Little, N Engl J Med, 1968). Cells will die within a few hours of irradiation exposure and begin to undergo nuclear breakdown and DNA degradation (Little, N Engl J Med, 1968). In HeLa cells, x-ray irradiation exposure resulted in an increase in reactive oxygen species, DNA double stranded breaks, apoptosis and lack of cell proliferation (Zhao *et al*., Oncol Lett, 2019). I found that irradiation increased the number of nuclei present and these are smaller in size in comparison to the undamaged samples. This data was also consistent when each time point was quantified separately. This suggests that irradiation is causing an effect at the cellular level and the variations in nuclear morphology can be attributed to damage caused by irradiation. One possibility to explain this is that irradiation induces proliferation. Proliferative conditions are stimulated in response to cytokines, which often occurs in response to damage or injury (Mukherjee *et al.*, Mech Ageing Dev, 2005). After irradiation, proliferative conditions are most likely occurring to replace the damaged cells, which could explain the increase in the number of nuclei in the irradiated samples. Alternatively, the smaller nuclei observed in the irradiated samples may be a consequence of nuclear fragmentation (Little, N Engl J Med, 1968). Further research in this area is warranted to determine the origin of the smaller nuclei visualized—whether they are a consequence of cellular proliferation or cellular breakdown. Proliferation could be tested by labelling proliferating cells and using a reagent such as Bromodeoxyuridine (BrdU) labelling to label S-Phase cells, or phosphor-HistoneH3 to label

dividing mitotic cells. This would provide insight into the regenerative response process following irradiation damage.

The intestinal epithelium is a barrier against chemicals, pathogens and bacteria (Ayyaz & Jasper, Front Cell Infect Microbiol, 2013). The disruptions to the intestinal epithelium can result in intestinal dysbiosis and inflammation (Ayyaz & Jasper, Front Cell Infect Microbiol, 2013). This makes the intestine leaky, permeable to biomolecules and pathogens. The effects of irradiation on intestinal permeability was tested using the Smurf assay. In this assay, control flies were fed a solution of bromophenol blue 48-hours prior to irradiation at ZT0 (7:00a.m.), causing their intestine to turn blue. Due to the relatively transparent nature of the *Drosophila melanogaster* abdomen, the intestines can be visualized while the fly is still living. Under normal conditions, the blue dye is localized to the intestine and the digestive tract can be visualized, but if the dye passes the intestinal barrier, it stains the body cavity blue as well. It was discovered that irradiated flies exhibited either intermediate or full levels of 'smurfness', whereas the control flies all exhibited no 'smurfness'. This shows that irradiation causes intestinal leakiness. As a consequence, bacteria and other harmful pathogens might pass through the intestinal epithelium, allowing for the potential development of infection (Peterson & Artis, Nat Rev Immunol, 2014). In this study, I only tested flies at one time of day. However, this response might be time-dependent or regulated by the circadian clock. Further research can investigate the levels of 'smurfness' after flies are irradiated at different times of day. This will provide insight whether time of day variations have an effect on the level of intestinal leakiness. Testing circadian clock mutants, like PER, would determine if the circadian clock regulates this response.

4.2 JAK/STAT Stress Response Pathway is Under Clock Control

JAK/STAT has an integral role in maintaining tissue homeostasis through cellular proliferation and differentiation. Baseline levels of JAK/STAT activity are expected to be present in an intestinal stem cell (Jiang *et al.*, Cell, 2009; Beebe *et al.*, Dev Biol, 2010) to differentiate cells of the enterocyte lineage (Beebe *et al.*, Dev Biol, 2010). Following damage, JAK/STAT activity levels would increase as stem cells transition to rapid proliferation to quickly replace the damaged cells. I found that irradiation damage resulted in increased JAK/STAT activity levels at three-hours post irradiation.

I first determined that under undamaged conditions the JAK/STAT pathway is regulated by the clock gene, PER, in a non-time dependent manner. This means that the levels of JAK/STAT activity are regulated by PER, and mutations in PER result in suppressed levels of JAK/STAT activity in comparison to the control flies. I then tested JAK/STAT activity after irradiation. JAK/STAT response in the control flies varied depending on the time of day irradiation was administered. JAK/STAT activity was most responsive when the control flies were irradiated at 1:00a.m., and least responsive when irradiated at 1:00p.m. Research by Lee and Edery (Curr Biol, 2008) as well as Kuo and colleagues (BMC Neurosci, 2010) found that the *Drosophila* survival rate is lower when damage by pathogen infection occurs during the daytime in comparison to being infected at nighttime. As such, the findings of my research could suggest that the variation in survival, as researched in the aforementioned studies, could be attributed to the time dependent changes in the JAK/STAT activity levels, whereby the flies irradiated during the nighttime had increased JAK/STAT activity levels and the flies irradiated during the daytime had decreased JAK/STAT activity levels. Under damaging conditions, injured cells are quickly replaced with new cells implicating the importance of the proliferative role of JAK/STAT

activity to regenerate the intestine (Jiang *et al.*, Cell, 2009). I believe that the time dependent variations in JAK/STAT cellular proliferation have a direct effect on the survival rates of the flies, making them more or less responsive to the damage depending on the time of day the damage occurs. These time of day differences were not seen in the clock mutant, which supports the notion that the circadian clock regulates JAK/STAT activity. Therefore, the JAK/STAT stress response appears to be most responsive to injury when the damage is inflicted in the early morning hours. Therefore, this finding is of importance because it illustrates the significance of the relationship between the JAK/STAT pathway response and the circadian clock.

It is possible that the JAK/STAT pathway may be under clock control either cell intrinsically or extrinsically of intestinal stem cells. Cell intrinsic factors of the JAK/STAT pathway that may be controlled by the clock could include any step that is occurring in the JAK/STAT pathway process within the cell's cytoplasm, such as the phosphorylation of JAK substrates or the dimerization of the STAT molecules, for example. Additionally, stem cell related intrinsic factors could also be regulated by the clock. This could include the initiation of the signaling cascade, such as the strength of the binding affinity between the ligand and its cytokine binding receptor or the potential of the transcription factors to effectively bind to the promoter to promote the transcription of the various target genes. Activation of the JAK/STAT pathway via UPD cytokine ligands is an extrinsic factor that may be controlled by the clock. Another possibility through which the JAK/STAT pathway may be controlled by the clock is behaviourally, such as entrainment to food. Additional testing will need to be conducted to further explore the mechanism or combination of mechanisms that are in play. For example, conducting a food timing assay to determine if the JAK/STAT pathway is controlled by the clock behaviourally. In this assay, flies are starved of nutrients for a certain period of time in order to

identify the effects of food and determine if the trends I observed continue to persist when flies are deprived of food, because food may be an external cue for the clock. If the trends persist in the absence of food, it could indicate that the trends observed are controlled by the clock. If the trends are not present in the absence of food, it may suggest that the JAK/STAT pathway is not controlled by the clock and instead, food may be a strong zeitgeber cue.

Along with the JAK/STAT pathway, the JNK pathway and the Hippo pathway also have a role in the stress response (Zeke *et al*., Microbiol Mol Biol R, 2016). The Hippo pathway reporter I tested did not work and so it was not used in the rest of this study. The JNK reporter was tested in a similar fashion as the JAK/STAT reporter but did not show a time-dependent response. It is possible that the x-ray irradiation was not a strong enough damaging agent to elicit a JNK pathway response. Another possibility is that the JNK pathway may not be directly involved in the acute damage stress response system. Instead, it may act as an additional supplementary pathway that is involved in the stress response, as it is known to be in frequent communication with many other cell signaling pathways involved in the stress response (Zeke *et al*., Microbiol Mol Biol R, 2016). Future studies should verify the effectiveness of the JNK and YKI reporter strains, using reverse transcriptase quantitative polymerase chain reaction (RT-qPCR) to accurately assess the transcriptional reporter activity readout. RT-qPCR provides a measure of gene expression by determining the amount of messenger ribonucleic acid (RNA) present (Taylor *et al.*, Trends Biotechnol, 2019) within the intestinal tissue being sampled. qPCR will amplify the gene that is being driven by the reporter (Taylor *et al.*, Trends Biotechnol, 2019), to verify if the reporter is functioning properly.

One of the characteristics of circadian rhythms is the ability to persist under free-running conditions (DD). In the absence of external time cues, the rhythms observed are a result of

previous entrainment of the endogenous time-keeper by external cues such as light/dark cycles or food (Duboway & Sehgal, Genetics, 2017). In this thesis, I have performed only circadian experiments under DD conditions to determine if the time-dependent activity observed is actually circadian in nature. By also using the PER mutant, I have performed experiments that confirm the circadian clock is responsible for the time of day changes observed.

4.3 Bacterial Presence Is Required to Elicit a Stress Response

Drosophila have evolved a robust defense mechanism against microbes. This is particularly important for their survival because they are constantly feeding on rotting and decaying fruit (Apidianakis & Rahme, Dis Model Mech, 2011). *Drosophila* and their microbiota have evolved into a commensal relationship together. Intestinal stress after irradiation could be a result of the damage caused by x-ray or an inflammatory response caused by increased bacterial presence following damage (Apidianakis & Rahme, Dis Model Mech, 2011). To be able to decipher the origin of the intestinal stress, I tested if intestinal bacteria are required to elicit a JAK/STAT response.

Axenic (no bacteria) flies had zero GFP+ cells (indicative of JAK/STAT activity). This is a critical finding because it shows the bacteria are required in order for the JAK/STAT pathway to elicit a response. Therefore, it was found that bacterial presence is necessary for JAK/STAT activity to occur. A future experiment is to complete this assay at additional time points to ascertain that the trends observed are consistent throughout the entire day. Additional time points would provide a better resolution to the possible role of circadian influences with respect to bacterial presence because the effects of the circadian rhythm may be fluctuating throughout the day, but its effects may be masked due to the limited time points observed. It is

anticipated that even with additional time points, that the data will be consistent with the axenic assay conducted, using minimal time points, hence the requirement of bacteria to elicit a JAK/STAT response.

Production of reactive oxygen species and superoxide molecules in the intestine are normal physiological processes as a consequence of mitochondrial aerobic metabolism (Miwa *et al.,* Free Radic Biol Med, 2003). Reactive oxygen species are harmful because they are unstable and highly reactive molecules (Vaccaro *et al*., Cell, 2020). In attempt to stabilize their own structure, reactive oxygen species will take electrons from DNA and other macromolecules rendering them to become unstable (Vaccaro *et al*., Cell, 2020). Increased levels of reactive oxygen species and superoxides have been linked to decreased survival in *Drosophila* (Vaccaro *et al*., Cell, 2020) as well as some neurological disorders (Oswald *et al.,* eLife, 2018). I investigated if x-ray irradiation damage could cause an increase in the levels of reactive oxygen species and superoxide production, and if so, determine if there is time dependence on the production of these molecules.

To do this I used DHE dye, a cytosolic and nuclear staining dye that fluoresces red when it reacts with reactive oxygen species (Owusu-Ansah *et al.,* Protec Exch, 2008). DHE staining was not consistent between samples, for some, the DHE would clearly stain the cells whereas in other samples, there was increased background staining. To circumvent this, the DHE+ cells within the R5 region were individually circled and an individual intensity value for the circled cell was established. I determined that time of day variation in superoxide presence is not statistically significant in either undamaged or irradiated conditions. Actually, irradiation damage did not increase the number of superoxide molecules present in comparison to the controls. This data corroborates previously published literature by Azzam and colleagues

(Cancer Lett, 2012) which shows that the levels of ROS produced as a result of irradiation damage are similar to the levels of endogenously produced ROS. My data does not show that reactive oxygen species increase following damage.

Additionally, recent research by Ulgherait and colleagues (Nat Commun, 2020) shows that a clock mutation in a period gene will induce increased mitochondrial uncoupling. When subjected to injury or damage, organisms can undergo mitochondrial uncoupling as a protective mechanism to prevent cellular degradation caused by increased ROS levels (Mookerjee *et al.*, Mech Ageing Dev, 2010). The electron transport chain is not used in mitochondrial uncoupling. Instead, other cellular processes allow protons to enter the extracellular matrix, bypassing the electron transport chain (Mookerjee *et al.*, Mech Ageing Dev, 2010), which results in decreased endogenous ROS production. When comparing the ratio levels of DHE+ cells to the total cells in the undamaged group and the irradiated group, it is observed that the number of DHE+ cells in the irradiated control samples are less than the number of DHE+ cells in the undamaged control samples. Similar to the reduced presence of superoxides in the period clock mutants, mitochondrial uncoupling may be reducing the overall presence of ROS in irradiated flies, which could be a possible explanation as to why superoxide presence was not increased following irradiation.

A possible limitation is that dissecting the intestines three-hours post irradiation may not have been enough time to observe exogenous reactive oxygen species generation caused by x-ray irradiation. As mentioned previously, the DHE dye was not very specific in its staining, so future research could involve using a different superoxide stain (such as Cy3) and testing at different times of day to provide further tests of superoxide presence. Investigating the role of superoxide presence can provide insight into any time dependent stress responses of the cell.

4.4 There is No Clock Dependence on the JAK/STAT Pathway

My research focused on the regulation of the stress response by the circadian clock, and I found that JAK/STAT signaling was time and PER dependent. To test the reverse, if JAK/STAT could regulate the circadian clock, the pathway was activated using its ligand UPD cytokine and studied using a clock reporter background.

The anterior region (R1), the middle region (R2, R3 and R4), the posterior region (R5) and the entire intestine (R1 to R5) were tested separately. All these regions have similar rhythms. The unpaired overexpression groups all peak at ZT0 (7:00a.m.) and trough at around ZT12/ZT15 (7:00p.m./10:00p.m.). The control groups have a dampened rhythm but all the graphs peak at around ZT0/ZT3 (7:00a.m./10:00a.m.) and trough at around ZT6 (1:00p.m.) and then again at around ZT15 (10:00p.m.).

The rhythm observed in the unpaired overexpression groups matches the clock reporter rhythm that was previously determined in our lab (Parasram *et al.*, Stem Cell Rep, 2018). However, the dampened control rhythms in Figures 20 B – E do not match the published data. This discrepancy could have been a technical issue, and needs to be revisited to confirm. However, my data suggests that the clock does not have dependence on the JAK/STAT pathway because regardless of control or UPD overexpression conditions, the clock reporter rhythm remained unchanged, suggesting that the JAK/STAT pathway is not upstream of clock signaling. If the clock was dependent on the JAK/STAT pathway, a different rhythm could have been observed under UPD overexpression conditions. This data complements the findings suggested by Luo and colleagues (Cell, 2012) that the circadian clock neurons are upstream of JAK/STAT signaling.

Overall a major finding from this work is that the circadian clock regulates the JAK/STAT stress response pathway. Additionally, I discovered that the presence of bacteria is required to elicit JAK/STAT activity. The mechanism I suggest for the data I obtained is illustrated in Figure 23B. I propose that following irradiation damage, the *Drosophila* intestine becomes damaged, which results in increased intestinal leakiness and increased changes in nuclear morphology. Consequently, bacteria and other pathogens will have facilitated access to enter the intestine. In turn, the intestine will become inflamed, causing increased JAK/STAT signaling activity (Figure 23A). Additionally, my research suggests that the JAK/STAT signaling pathway is a downstream of the circadian clock, which would indicate that the JAK/STAT pathway is regulated by the circadian clock (Figure 23B). Future studies can further explore the precise mechanism between the JAK/STAT pathway and the circadian clock. The JAK/STAT pathway is evolutionarily conserved between organisms, and this research may also aid in combating infections and diseases when treatments are administered at times in which the response to damage is most effective.

FIGURE 23:

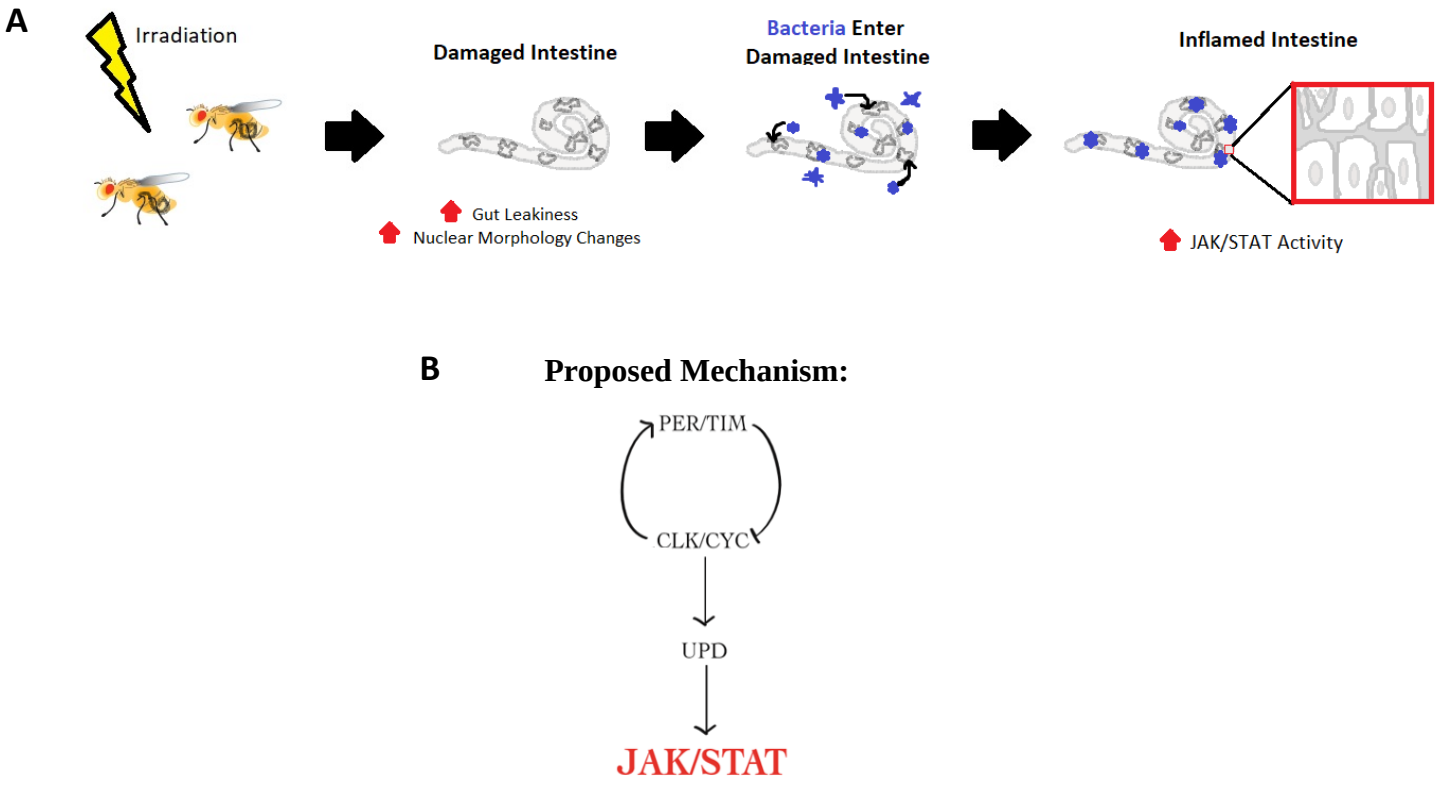

Figure 23: Concluding Graphical Abstract (A) and Proposed Mechanism (B)

REFERENCES

1. Agaisse H and Perrimon N (2004) The roles of JAK/STAT signaling in *Drosophila* immune responses. Immunol Rev *198, 72-82*
2. Allada R and Chung BY (2010) Circadian organization of behavior and physiology in *Drosophila.* Annu Rev Physiol *72*, 605-624
3. Amcheslavsky A, Jiang J and Ip Ty (2009) Tissue-damage induced intestinal stem cell division in *Drosophila.* Cell Stem Cell *4*(1), 49-61 DOI: doi: 10.1016/j.stem.2008.10.016
4. Apidianakis Y and Rahme LG (2011) *Drosophila melanogaster* as a model for human intestinal infection and pathology. Dis Model Mech *4*(1), 21-30
5. Arbouzova NI and Zeidler MP (2006) JAK/STAT signaling in *Drosophila*: insights into conserved regulatory and cellular functions. Dev (Review) *133*, 2605-2616
6. Ayyaz A and Jasper H (2013) Intestinal inflammation and stem cell homeostasis in aging *Drosophila melanogaster*. Front Cell Infect Microbiol DOI: https://doi.org/10.3389/fcimb.2013.00098
7. Azzam EI, Jay-Gerin JP and Pain, D (2012) Ionizing radiation-induced metabolic oxidative stress and prolonged cell injury. Cancer Lett *327*(1-2), 48-60
8. Baik LS, Au DD, Nave C, Foden AJ, Enriqquez-Villalva WK and Holmes TC (2019) Distinct mechanisms of *Drosophila* Cryptochrome-mediated light-evoked membrane depolarization and in vivo clock resetting. PNAS *116*(46), 23339-23344
9. Beebe K, Lee WL and Micchelli CA (2010) JAK/STAT signaling coordinates stem cell proliferation and multilineage differentiation in the *Drosophila* intestinal stem cell lineage. Dev Bio *338*, 28-37

10. Biteau B, Hichmuth C and Jasper H (2011) Maintaining tissue homeostasis: dynamic control of somatic stem cell activity. Cell Stem Cell (Review) *9*, 402-411
11. Boopathy GTK and Hong W (2019) Role of Hippo-pathway YAP/TAZ signaling in angiogenesis. Front Cell Dev Biol *10*(7), DOI: doi: 10.3389/fcell.2019.00049
12. Booth C, Tudor G, Tudor J, Katz BP and MacVittie T (2012) The acute gastrointestinal syndrome in high-dose irradiated mice. Health Phys *103*(4), 383-399
13. Brenman-Suttner DB, Long SQ, Kamesan V, de Belle JN, Yost RT, Kanippayoor RL and Simon AF (2018) Progeny of old parents have increased social space in *Drosophila melanogaster*. Scientific Reports. *8*(3673) DOI: doi:10.1038/s41598-018-21731-0
14. Buchon N, Broderick NA, Poidevin M, Pradervand S and Lemaitre, B (2009) *Drosophila* intestinal response to bacterial infection: activation of host defense and stem cell proliferation. Cell Host Microbe *5*(2), 200-211
15. Buchon N, Osman D, David FP, Fang HY, Boquete JP, Deplancke B and Lemaitre B (2013) Morphological and molecular characterization of adult midgut compartmentalization in *Drosophila*. Cell Reports *3*, 1725-1738
16. Busza A, Emery-Le M, Rosbach M and Emery P (2004) Roles of the two *Drosophila* CRYPTOCHROME Structural Domains in Circadian Photoreception. Science *304*(5676), 1503-1506
17. Capo F, Wilson A and Di Cara F (2019) The intestine of *Drosophila melanogaster*: an emerging versatile model system to study intestinal epithelial homeostasis and host-microbial interactions in humans. Microorganisms *7*(9), 336 DOI: https://doi.org/10.3390/microoganisms7090336

18. Castillo MR, Hochstetler KJ, Tavernier Jr RJ, Greene DM and Bult-Ito A (2004) Entrainment of the master circadian clock by scheduled feeding. Am J Physiol-Reg I *287*(3), R551-R555
19. Czeisler CA, Duffy JF, Shanahan TL, Brown EN, Mitchel JF, Rimmer DW… Kronauer RE (1999) Stability, precision, and near-24-hour period of the human circadian pacemaker. SCIEAS *284*(5423), 2177-2181
20. Dubowy C and Sehgal A (2017) Circadian rhythms and sleep in *Drosophila melanogaster*. Genetics *205*(4), 1373-1397
21. Farhud D and Aryan Z (2018) Circadian rhythm, lifestyle and health: a narrative review. Iran J Public Health *47*(8), 1068-1076
22. Fernandez-Moreno MA, Farr CL, Kaguni LS and Garesse R (2007) *Drosophila melanogaster* as a model system to study mitochondrial biology. Methods Mol Biol *372*, 33-49
23. Ferree PL, Deneke VE and DiTalia S (2016) Measuring time during early embryonic development. Semin Cell Dev Biol 55, 80-88
24. Fujimoto E, Gaynes B, Brimley C, Chien CB and Bonkowsky J (2011) Gal80 intersectional regulation of cell-type specific expression in vertebrates. Developmental Dynamics. *240*(10), 2324-2334
25. Gale JE, Cox HI, Qian J, Block GD, Colwell CS and Matveyenko (2011) Disruption of circadian rhythms accelerates development of diabetes through beta-cell loss and dysfunction. J Biol Rhythms *26*(5), 423-433

26. Halberg F, Johnson EA, Brown BW and Bittner JJ (1960) Susceptibility rhythm to E. coli endotoxin and bioassay. Exp Biol Med DOI: https://doi.org/10.3181/00379727-103-25439

27. Hardin, P (2011) Molecular genetic analysis of circadian timekeeping in *Drosophila*. Adv Genet *74*, 141-173

28. He L, Binari R, Huang J, Falo-Sanjuan J and Perrimon N (2019) In vivo study of gene expression with an enhanced dual-color fluorescent transcriptional timer. eLife 2019;8:e46181 DOI: doi:10.7554/eLife.46181

29. Herrera SC and Bach EA (2018) JAK/STAT signaling in stem cells and regeneration: from *Drosophila* to vertebrates. Development *146,* dev167643 DOI: doi: 10.1242/dev.167643

30. Hung RJ, Hu Y, Kirchner R, Liu Y, Xu C, Comjean A … Perrimon, N (2020) A cell atlas of the adult *Drosophila* midgut. PNAS *117*(3), 1514-1523

31. Iatsenko I, Boquete JP and Lemaitre B (2018) Microbiota-derived lactate activates production of reactive oxygen species by the intestinal NADPH oxidase Nox and shortens *Drosophila* lifespan. Immunity *49*(5): 929-942

32. Jiang H, Patel P, Kohlmaier A, Grenley M, McEwen D and Edgar B (2009) Cytokine/Jak/Stat signaling mediates regeneration and homeostasis in the *Drosophila* midgut. Cell *137*, 1343-1355

33. Karpowicz P, Zhang Y, Hogenesch JB, Emery P and Perrimon N (2013) The circadian clock gates the intestinal stem cell regenerative state. Cell Rep *3,* 996-1004

34. Klarsfeld A and Rouyer F (1998) Effects of circadian mutations and LD periodicity on the lifespan of *Drosophila melanogaster*. J Biol Rhythm *13*(6), 471-478

35. Krishnan N, Kretzschmar D, Rakshit K, Chow E and Giebultowicz JM (2009) The circadian clock gene *period* extends healthspan in aging *Drosophila melanogaster.* Aging Albany NY *1*(11), 937-948

36. Kuo TH, Pike DH, Beizaeipour Z and Williams JA (2010) Sleep triggered by an immune response in *Drosophila* is regulated by the circadian clock and requires the NFκB relish. BMC Neurosci *11*(17), DOI: https://doi.org/10.1186/1471-2202-11-17

37. Lee C, Bae K and Edery I (1999) PER and TIM inhibit the DNA binding activity of a *Drosophila* CLOCK-CYC/dBMAL1 heterodimer without disrupting formation of the heterodimer: a basis for circadian transcription. Mol Cell Biol *19*(8), 5316- 5325

38. Lee JE and Edery I (2008) Circadian regulation in the ability of *Drosophila* to combat pathogenic infection. Curr Biol *18*(3), 195-199

39. Lin G, Xu N and Xi R (2010) Paracrine unpaired signaling through the JAK/STAT pathway controls self-renewal and lineage differentiation of *Drosophila* intestinal stem cells. J Mol Cell Biol *2*(1), 37-49

40. Linford NJ, Bilgir C, Ro J and Pletcher SD (2013) Measurement of lifespan in *Drosophila melanogaster*. J Vis Exp 71: 50068 DOI: doi: 10.3791/50068

41. Little JB (1968) Cellular effects if ionizing radiation. N Engl J Med *278*(7), 369-376

42. Luo W and Sehgal A (2012) Regulation of circadian behavioural output via a micro-RNA JAK/STAT circuit. Cell DOI: doi: https://doi.org/10.1016/j.cell.2011.12.024

43. Marianes A and Spradling AC (2013) Physiological and stem cell compartmentalization within the *Drosophila* midgut. eLife *2*: e00886 DOI: doi: 10.7554/eLife.00886

44. Martins RR, McCracken AW, Simons MJP, Henriques CM and Rera M (2018) How to catch a Smurf? – Ageing and beyond… *In vivo* assessment of intestinal permeability in multiple model organisms. Bio Protec *8*(3), e2722
45. McHill AW, Butler MP and Shea SA (2017) Free-Running Cycle. Encyclopedia of Animal Cognition and Behaviour: Living Edition. DOI: https://doi.org/10.1007/978-3-319-47829-6_1942-1
46. Micchelli CA and Perrimon N (2006) Evidence that stem cells reside in the adult *Drosophila* midgut epithelium. Nature (Letters) *439*, 475-479
47. Miwa S, St. Pierre J, Partridge L and Brand MD (2003) Superoxide and hydrogen oxide production by *Drosophila* mitochondria. Free Radic Biol Med *35*(8), 938-948
48. Mookerjee SA, Divakaruni AS, Jastroch M and Brand MD (2010) Mitochondrial uncoupling and lifespan. Mech Ageing Dev *131*(7-8), 463-472
49. Muller P, Kuttenkeuler D, Gesellchen V, Zeidler M and Boutros M (2005) Identification of JAK/STAT signaling components by genome-wide RNA interference. Nature *436*(7052), 871-875
50. Myers MP, Wager-Smith K, Wesley CS, Young MW and Seghal A (1995) Positional cloning and sequence analysis of the *Drosophila* clock gene, timeless. Science 270(5237), 805-808
51. Ohlstein B and Spradling A (2006) The adult *Drosophila* posterior midgut is maintained by pluripotent stem cells. Nature (Letters) *439*, 470-474
52. Ong C, Yung LY, Cai Y, Bay BH and Baeg GH (2015) *Drosophila melanogaster* as a model organism to study nanotoxicity. Nanotoxicity 9(3), 396-403

53. Oswald MCW, Brooks PS, Zwart MF, Mukherjee A, West RJH, Giachello CNG … Sweeney ST (2018) Reactive oxygen species regulate activity-dependent neuronal plasticity in *Drosophila.* eLife DOI: doi: 10.7554/eLife.39393

54. Owusu-Ansah E, Yavari A and Banerjee U (2008) A protocol for *in vivo* detection of reactive oxygen species. Protoc Exch DOI: doi:10.1038/n.prot.2008.23

55. Panayidou S and Apidianakis Y (2013) Regenerative inflammation: lessons from *Drosophila* intestinal epithelium in health and disease. Pathogens *2*(2), 209-231

56. Panda S, Hogenesch J and Kay S (2002) Circadian rhythm from flies to human. Nature *417*, 329-335

57. Parasram K, Bernardon N, Hammoud M, Chang H, He L, Perrimon N and Karpowicz P (2018) Intestinal stem cells exhibit conditional circadian clock function. Stem Cell Rep *11*(5), 1287-1301

58. Parasram K and Karpowicz P (2019) Time after time: circadian clock regulation of intestinal stem cells. Cell Mol Life Sci *77*(7), 1267-1288

59. Peterson LW and Artis D (2014) Intestinal epithelial cells: regulators of barrier function and immune homeostasis. Nat Rev Immunol *14*, 141-153

60. Savvidis C and Koutsilieris M (2012) Circadian disruption in cancer biology. Mol Med 18, 1249-1260

61. Serin Y & Acar Tek N (2019) Effect of circadian rhythm on metabolic processes and the regulation of energy balance. Ann Nutr Metab *74*(4), DOI: https://doi.org/10.1159/000500071

62. Spiegel K, Leproult R and Van Cauter E (1999) Impact of sleep debt on metabolic and endocrine function. The Lancet *354*(9188), 1435-1439

63. Stone EF, Fulton BO, Ayres JS, Pham LN, Ziauddin J and Shirasu-Hiza M (2012) The circadian clock protein timeless regulates phagocytosis of bacteria in *Drosophila.* PLoS Path, DOI: https://doi.org/10.1371/journal.ppat.1002445

64. Takada S, Kelkar A and Theurkauf WE (2003) Drosophila checkpoint kinase 2 couples centrosome function and spindle assembly to genomic integrity. Cell 113, 87–99

65. Takashima S, Mkrtchyan M, Younossi-Hartenstein A, Merriam JR and Hartenstein V (2008) The behavior of *Drosophila* adult hindgut stem cells is controlled by Wnt and Hh signaling. Nature *454*, 651-655

66. Taylor SC, Nadeau K, Abbasi M, Lachance C, Nguyen, M and Fenrich J (2019) The ultimate qPCR experiment: producing publication quality, reproducible data for the first time. Trends Biotechnol *37*(7), 761-774

67. Ulgherait M, Chen A, McAllister SF, Kim HX, Delventhal R, Wayne CR…Shirasu-Hisa M (2020) Circadian regulation of mitochondrial uncoupling and lifespan. Nat Commun *11*, DOI: https://doi.org/10.1038/s41467-020-15617-x

68. Vaccaro A, Kaplan Dor Y, Nambara K, Pollina EA, Lin C, Greenberg ME and Rogulja D (2020) Sleep loss can cause death through accumulation of reactive oxygen species in the gut. Cell DOI: https://doi.org/10.1016/j.cell.2020.04.049

69. Verghese S and Su TT (2016) *Drosophila* Wnt and STAT define apoptosis-resilient epithelial cells for tissue regeneration after irradiation. PLoS Biol *14*(9): e1002536 DOI: doi: 10.1371/journal/pbio.1002536

70. Wang Y and Zhong Y (2004) TARGETing “When” and “Where”. [Perspective] Science *200* DOI: doi: 10.1126/stke.2202004pe5

71. Yamaguchi M and Kashiwakura I (2013) Role of reactive oxygen species in the radiation response of human hematopoietic stem/progenitor cells. PLoS One, DOI: https://doi.org/10.1371/journal.pone.0070503

72. Yoshii T, Hermann-Luibl C, Kistenpfennig C, Schmid B, Tomioka K and Helfrich-Forster C (2015) Cryptochrome-dependent and –independent circadian entrainment circuits in *Drosophila.* J Neurosci *35*(15), 6131-6141

73. Zeke A, Misheva M, Remenyi A and Bogoyevitch MA (2016) JNK Signaling: regulation and function based on complex protein-protein partnerships. Microbiol Mol Biol R *80*(3), 793-835

74. Zhao H, Zhuang Y, Li R, Liu Y, Mei Z, He Z … Zhou Y (2019) Effects of different doses of x-ray irradiation on cell apoptosis, cell cycle, DNA damage repair and glycolysis in HeLa cells. Oncol Lett *17*(1), 42-54

VITA AUCTORIS

NAME:	Daniela Bianca Bachetti
PLACE OF BIRTH:	Windsor, Ontario, Canada
YEAR OF BIRTH:	1995
EDUCATION:	University of Windsor, Windsor, Ontario, Canada B.Sc.(H) 2013-2017
	St. Joseph Catholic High School, Windsor, Ontario, Canada 2009-2013